



1 The ABCflux database: Arctic-Boreal CO<sub>2</sub> flux  
2 observations and ancillary information aggregated to  
3 monthly time steps across terrestrial ecosystems

4  
5 Authors: Anna-Maria Virkkala<sup>1</sup>, Susan M. Natali<sup>1</sup>, Brendan M. Rogers<sup>1</sup>, Jennifer D. Watts<sup>1</sup>,  
6 Kathleen Savage<sup>1</sup>, Sara June Connon<sup>1</sup>, Marguerite Mauritz<sup>2</sup>, Edward A.G. Schuur<sup>3</sup>, Darcy Peter<sup>1</sup>,  
7 Christina Minions<sup>1</sup>, Julia Nojeim<sup>1</sup>, Roisin Commane<sup>4</sup>, Craig A. Emmerton<sup>5</sup>, Mathias Goeckede<sup>6</sup>,  
8 Manuel Helbig<sup>7,8</sup>, David Holl<sup>9</sup>, Hiroki Iwata<sup>10</sup>, Hideki Kobayashi<sup>11</sup>, Pasi Kolari<sup>12</sup>, Efrén López-  
9 Blanco<sup>13,14</sup>, Maija E. Marushchak<sup>15,16</sup>, Mikhail Mastepanov<sup>14,17</sup>, Lutz Merbold<sup>18</sup>, Frans-Jan W.  
10 Parmentier<sup>19,20</sup>, Matthias Peichl<sup>21</sup>, Torsten Sachs<sup>22</sup>, Oliver Sonnentag<sup>8</sup>, Masahito Ueyama<sup>23</sup>,  
11 Carolina Voigt<sup>15,8</sup>, Mika Aurela<sup>24</sup>, Julia Boike<sup>25,26</sup>, Gerardo Celis<sup>27</sup>, Namyi Chae<sup>28</sup>, Torben R.  
12 Christensen<sup>14</sup>, M. Syndonia Bret-Harte<sup>29</sup>, Sigrid Dengel<sup>30</sup>, Han Dolman<sup>31</sup>, Colin W. Edgar<sup>29</sup>, Bo  
13 Elberling<sup>32</sup>, Eugenie Euskirchen<sup>29</sup>, Achim Grelle<sup>33</sup>, Juha Hatakka<sup>24</sup>, Elyn Humphreys<sup>34</sup>, Järvi  
14 Järveoja<sup>21</sup>, Ayumi Kotani<sup>35</sup>, Lars Kutzbach<sup>9</sup>, Tuomas Laurila<sup>24</sup>, Annalea Lohila<sup>24,12</sup>, Ivan  
15 Mammarella<sup>12</sup>, Yojiro Matsuura<sup>36</sup>, Gesa Meyer<sup>8,37</sup>, Mats B. Nilsson<sup>21</sup>, Steven F. Oberbauer<sup>38</sup>,  
16 Sang-Jong Park<sup>39</sup>, Roman Petrov<sup>40</sup>, Anatoly S. Prokushkin<sup>41</sup>, Christopher Schulze<sup>8,42</sup>, Vincent L.  
17 St.Louis<sup>5</sup>, Eeva-Stiina Tuittila<sup>43</sup>, Juha-Pekka Tuovinen<sup>24</sup>, William Quinton<sup>44</sup>, Andrej Varlagin<sup>45</sup>,  
18 Donatella Zona<sup>46</sup>, Viacheslav I. Zyrjanov<sup>41</sup>

19

20

21 1 Woodwell Climate Research Center, 149 Woods Hole Road Falmouth, MA, 02540-1644, USA

22 2 University of Texas, at El Paso, 500 W University Rd, El Paso, TX 79902, USA

23 3 Center for Ecosystem Science and Society, and Department of Biological Sciences, Northern  
24 Arizona University, Flagstaff, AZ, 86001

25 4 Dept. of Earth & Environmental Sciences, Lamont-Doherty Earth Observatory, Columbia  
26 University, Palisades, NY 10964

27 5 Department of Biological Sciences, University of Alberta, Edmonton, Alberta, Canada T6G  
28 2E9

29 6 Dept. Biogeochemical Signals, Max Planck Institute for Biogeochemistry, Jena, Germany

30 7 Department of Physics and Atmospheric Science, Dalhousie University, Halifax, Nova Scotia,  
31 Canada

32 8 Departement de Geographie, Universite de Montreal, Montreal, Quebec, Canada



- 33 9 Institute of Soil Science, Center for Earth System Research and Sustainability (CEN),  
34 Universität Hamburg, Hamburg, Germany  
35 10 Department of Environmental Science, Shinshu University, Matsumoto, Japan  
36 11 Research Institute for Global Change, Japan Agency for Marine-Earth Science and  
37 Technology, Yokohama, Japan  
38 12 Institute for Atmospheric and Earth System Research/Physics, Faculty of Science, University  
39 of Helsinki, Finland  
40 13 Department of Environment and Minerals, Greenland Institute of Natural Resources, Kivioq  
41 2, 3900, Nuuk, Greenland  
42 14 Department of Bioscience, Arctic Research Center, Aarhus University, Frederiksborgvej 399,  
43 4000 Roskilde, Denmark  
44 15 Department of Environmental and Biological Sciences, University of Eastern Finland,  
45 Kuopio, Finland  
46 16 Department of Biological and Environmental Science, University of Jyväskylä, Jyväskylä,  
47 Finland  
48 17 Oulanka research station, University of Oulu, Liikasenvaarantie 134, 93900 Kuusamo,  
49 Finland  
50 18 Agroscope, Research Division Agroecology and Environment, Reckenholzstrasse 191, 8046  
51 Zurich, Switzerland  
52 19 Center for Biogeochemistry in the Anthropocene, Department of Geosciences, University of  
53 Oslo, 0315 Oslo, Norway  
54 20 Department of Physical Geography and Ecosystem Science, Lund University, 223 62 Lund,  
55 Sweden  
56 21 Department of Forest Ecology and Management, Swedish University of Agricultural  
57 Sciences, 901 83 Umeå, Sweden  
58 22 GFZ German Research Centre for Geosciences, Telegrafenberg, Potsdam, Germany  
59 23 Graduate School of Life and Environmental Sciences, Osaka Prefecture University, 1-1  
60 Gakuencho, Naka-ku, Sakai, 599-8531, Japan  
61 24 Finnish Meteorological Institute, Climate system research, Helsinki, Finland  
62 25 Alfred Wegener Institute Helmholtz Center for Polar and Marine Research, Telegrafenberg  
63 A45, 14473 Potsdam, Germany & Geography Department, Humboldt-Universität zu Berlin,  
64 Unter den Linden 6, 10099 Berlin, Germany  
65 26 Geography Department, Humboldt-Universität zu Berlin, Berlin, Germany  
66 27 Agronomy Department, University of Florida, Gainesville, USA  
67 28 Institute of Life Science and Natural Resources, Korea University, 145 Anam-ro, Seongbuk-  
68 gu, Seoul, 02841, Republic of Korea  
69 29 Institute of Arctic Biology, University of Alaska Fairbanks, Fairbanks, AK 99775, USA  
70 30 Earth and Environmental Sciences Area. Lawrence Berkeley National Lab, Berkeley, CA  
71 94720, USA  
72 31 Department of Earth Sciences, VU University of Amsterdam, Amsterdam, The Netherlands  
73 32 Center for Permafrost, Department of Geosciences and Natural Resource Management,  
74 University of Copenhagen, Øster Voldgade 10  
75 33 Department of Ecology, Swedish University of Agricultural Sciences, Uppsala  
76 34 Department of Geography & Environmental Studies, Carleton University, 1125 Colonel By  
77 Dr. Ottawa, ON, K2B 5J5 Canada  
78 35 Graduate School of Bioagricultural Sciences, Nagoya University, Nagoya, Japan



79 36 Forestry and Forest Products Research Institute  
80 37 Environment and Climate Change Canada, Climate Research Division, Victoria, BC V8N  
81 1V8, Canada  
82 38 Department of Biological Sciences and Institute of Environment, Florida International  
83 University, Miami Florida 33199 USA  
84 39 Division of Atmospheric Sciences, Korea Polar Research Institute, 26 Songdomirae-ro  
85 Yeonsu-gu, Incheon, Republic of Korea 21990  
86 40 Institute for Biological Problems of Cryolithozone of the Siberian Branch of the RAS -  
87 Division of Federal Research Centre “The Yakut Scientific Centre of the Siberian Branch of the  
88 Russian Academy of Sciences  
89 41 VN Sukachev Institute of forest SB RAS, Akademgorodok 50/28, Krasnoyarsk 660036  
90 Russia  
91 42 Department of Renewable Resources, University of Alberta, Edmonton, Alberta, Canada  
92 T6G 2E9  
93 43 School of Forest Sciences, University of Eastern Finland, Finland  
94 44 Cold Regions Research Centre, Wilfrid Laurier University, Waterloo, Ontario, Canada, N2L  
95 3C5  
96 45 A.N. Severtsov Institute of Ecology and Evolution, Russian Academy of Sciences, 119071,  
97 Leninsky pr.33, Moscow, Russia  
98 46 Department of Biology, San Diego State University  
99  
100 ORCID iDs:  
101 AMV: 0000-0003-4877-2918  
102 SMN: 0000-0002-3010-2994  
103 BMR: 0000-0001-6711-8466  
104 MaM: 0000-0001-8733-9119  
105 EAGS: 0000-0002-1096-2436  
106 RC: 0000-0003-1373-1550  
107 MG: 0000-0003-2833-8401  
108 MH: 0000-0003-1996-8639  
109 DH: 0000-0002-9269-7030  
110 HI: 0000-0002-8962-8982  
111 HK: 0000-0001-9319-0621  
112 PK: 0000-0001-7271-633X  
113 ELB: 0000-0002-3796-8408  
114 MEM: 0000-0002-2308-5049  
115 MiM: 0000-0002-5543-0302  
116 LM: 0000-0003-4974-170X  
117 FJP: 0000-0003-2952-7706  
118 MP: 0000-0002-9940-5846  
119 TS: 0000-0002-9959-4771  
120 MU: 0000-0002-4000-4888  
121 CV: 0000-0001-8589-1428  
122 MA: 0000-0002-4046-7225  
123 JB: 0000-0002-5875-2112  
124 GC: 0000-0003-1265-4063



125 TRC: 0000-0002-4917-148X  
126 MSB: 0000-0001-5151-3947  
127 SD: 0000-0002-4774-9188  
128 CE: 0000-0002-7026-8358  
129 BE: 0000-0002-6023-885X  
130 SEE: 0000-0002-0848-4295  
131 AG: 0000-0003-3468-9419  
132 EH: 0000-0002-5397-2802  
133 JJ: 0000-0001-6317-660X  
134 AK: 0000-0003-0350-0775  
135 LK: /0000-0003-2631-2742  
136 TL: 0000-0002-1967-0624  
137 AL: 0000-0003-3541-672X  
138 IM: 0000-0002-8516-3356  
139 GM: 0000-0003-3199-5250  
140 MBN: 0000-0003-3765-6399  
141 SFO: 0000-0001-5404-1658  
142 SJP: 0000-0002-6944-6962  
143 RP: 0000-0002-6877-3902  
144 ASP: 0000-0001-8721-2142  
145 CS: 0000-0002-6579-0360  
146 VLStL: 0000-0001-5405-1522  
147 EST: 0000-0001-8861-3167  
148 JPT: 0000-0001-7857-036X  
149 WQ: 0000-0001-5707-4519  
150 DZ: 0000-0002-0003-4839  
151 VIZ: 0000-0002-1748-4801  
152 AV: 0000-0002-2549-5236  
153 CAE: 0000-0001-9511-9191  
154  
155 Word count: 9200 (abstract: 330, main text: 6400)  
156 Corresponding author: Anna-Maria Virkkala, avirkkala@woodwellclimate.org  
157

158

159

160

161



## 162 Abstract

163 Past efforts to synthesize and quantify the magnitude and change in carbon dioxide (CO<sub>2</sub>) fluxes in  
164 terrestrial ecosystems across the rapidly warming Arctic-Boreal Zone (ABZ) have provided valuable  
165 information, but were limited in their geographical and temporal coverage. Furthermore, these efforts  
166 have been based on data aggregated over varying time periods, often with only minimal site ancillary  
167 data, thus limiting their potential to be used in large-scale carbon budget assessments. To bridge these  
168 gaps, we developed a standardized monthly database of Arctic-Boreal CO<sub>2</sub> fluxes (ABCflux) that  
169 aggregates *in-situ* measurements of terrestrial net ecosystem CO<sub>2</sub> exchange and its derived partitioned  
170 component fluxes: gross primary productivity and ecosystem respiration. The data span from 1989 to  
171 2020 with over 70 supporting variables that describe key site conditions (e.g., vegetation and disturbance  
172 type), micrometeorological and environmental measurements (e.g., air and soil temperatures) and flux  
173 measurement techniques. Here, we describe these variables, the spatial and temporal distribution of  
174 observations, the main strengths and limitations of the database, and the potential research opportunities it  
175 enables. In total, ABCflux includes 244 sites and 6309 monthly observations; 136 sites and 2217 monthly  
176 observations represent tundra, and 108 sites and 4092 observations represent the boreal biome. The  
177 database includes fluxes estimated with chamber (19 % of the monthly observations), snow diffusion (3  
178 %) and eddy covariance (78 %) techniques. The largest number of observations were collected during the  
179 climatological summer (June-August; 32 %), and fewer observations were available for autumn  
180 (September-October; 25 %), winter (December-February; 18 %), and spring (March-May; 25 %).  
181 ABCflux can be used in a wide array of empirical, remote sensing and modeling studies to improve  
182 understanding of the regional and temporal variability in CO<sub>2</sub> fluxes, and to better estimate the terrestrial  
183 ABZ CO<sub>2</sub> budget. ABCflux is openly and freely available online  
184 (<https://doi.org/10.3334/ORNLDAAAC/1934>, Virkkala et al., 2021a).

185

186

187

188

189

190



191 1. Introduction

192

193 The Arctic-Boreal Zone (ABZ), comprising the northern tundra and boreal biomes, stores  
194 approximately half the global soil organic carbon pool (Hugelius et al., 2014; Tarnocai et al.,  
195 2009; Mishra et al., 2021). As indicated by this large carbon reservoir, the ABZ has acted as a  
196 carbon sink over the past millenia due to the cold climate and slow decomposition rates (Siewert  
197 et al., 2015; Hugelius et al., 2020; Gorham, 1991). However, these carbon stocks are increasingly  
198 vulnerable to climate change, which is occurring rapidly across the ABZ (Box et al., 2019). As a  
199 result, carbon is being lost from this reservoir to the atmosphere as carbon dioxide (CO<sub>2</sub>) through  
200 increased ecosystem respiration (Reco) (Schuur et al., 2015; Parker et al., 2015; Voigt et al.,  
201 2017). The impact of increased CO<sub>2</sub> emissions on global warming depends on the extent to  
202 which respiratory losses are offset by gross primary productivity (GPP), the vegetation uptake of  
203 atmospheric CO<sub>2</sub> via photosynthesis (McGuire et al., 2016; Cahoon et al., 2016).

204

205 Carbon dioxide flux measurements provide a means to monitor the net CO<sub>2</sub> balance (i.e., net  
206 ecosystem exchange; NEE, a balance between GPP and Reco) across time and space (Baldocchi,  
207 2008; Pavelka et al., 2018). There are three main techniques used to measure fluxes at the  
208 ecosystem level that represent fluxes from plants and soils: eddy covariance, automated and  
209 manual chambers, and snow diffusion methods (hereafter diffusion; for a comparison of the  
210 techniques, see Table 1 in McGuire et al. 2012). The eddy covariance technique estimates NEE  
211 at the ecosystem scale (ca. 0.01 to 1 km<sup>2</sup> footprint) at high temporal resolution (i.e., ½ hr) using  
212 nondestructive and automated measurements (Pastorello et al., 2020). Automated and manual  
213 chamber techniques measure NEE at fine spatial scales (< 1 m<sup>2</sup>) and in small-statured  
214 ecosystems, common in the tundra, where the chambers can fit over the whole plant community  
215 (Järveoja et al., 2018; López-Blanco et al., 2017). The diffusion technique can be used to  
216 measure the transport of CO<sub>2</sub> within a snowpack (Björkman et al., 2010b). The eddy covariance  
217 technique has been used globally for over three decades, and chamber and diffusion techniques  
218 for even longer.

219

220 Historically, the number and distribution of ABZ flux sites has been rather limited compared to  
221 observations in temperate regions (Baldocchi et al., 2018). Due to these data gaps, quantifying



222 the net annual CO<sub>2</sub> balance across the ABZ has posed a significant challenge (Natali et al., 2019;  
223 McGuire et al., 2016; Virkkala et al., 2021b). However, over the past decade, the availability of  
224 ABZ flux data has increased substantially. Many, but not all, of the ABZ eddy covariance sites  
225 are a part of broader networks, such as the global FLUXNET and regional AmeriFlux, Integrated  
226 Carbon Observation System (ICOS) and the European Fluxes Database Cluster (EuroFlux),  
227 where data are standardized and openly available (Paris et al., 2012; Novick et al., 2018;  
228 Pastorello et al., 2020). These networks primarily include flux and meteorological data, but do  
229 not often include other environmental descriptions such as soil carbon stocks, dominant plant  
230 species, or the disturbance history of a given site (but see, for example, BADM data in  
231 Ameriflux), which are important for understanding the controls on CO<sub>2</sub> fluxes. Moreover, even  
232 though some ABZ annual chamber measurements are included in the global soil respiration  
233 database (SRDB) (Jian et al., 2020), and in the continuous soil respiration database (COSORE)  
234 (Bond-Lamberty et al., 2020), standardized datasets providing ABZ CO<sub>2</sub> flux measurements  
235 from eddy covariance, chambers, and diffusion, along with comprehensive metadata, have been  
236 nonexistent. Such an effort would create potential for a more thorough understanding of ABZ  
237 CO<sub>2</sub> fluxes. Therefore, compiling these flux measurements and their supporting ancillary data  
238 into one database is clearly needed to support future modeling, remote sensing, and empirical  
239 data mining efforts.

240

241 Arctic-Boreal CO<sub>2</sub> fluxes have been previously synthesized in a handful of regional studies  
242 (Belshe et al., 2013; McGuire et al., 2012; Luyssaert et al., 2007; Baldocchi et al., 2018; Virkkala  
243 et al., 2018; Natali et al., 2019; Virkkala et al., 2021b) (Fig. 1 and Table 1). One of the main  
244 challenges in these previous efforts, in addition to the limited geographical coverage of ABZ  
245 sites and lack of environmental descriptions, has been the variability of the synthesized seasonal  
246 measurement periods. Most of these efforts have allowed the seasonal definitions and  
247 measurement periods to vary across the sites, creating uncertainty in the inter-site comparison of  
248 flux measurements. An alternative approach to define seasonality is to focus on standard time  
249 periods such as months (Natali et al., 2019). Although focusing on monthly fluxes may result in  
250 a small decrease in synthesizable data, because publications, particularly older ones, often  
251 provide seasonal rather than monthly flux estimates (see e.g., (Euskirchen et al., 2012; Nykänen  
252 et al., 2003; Björkman et al., 2010a; Oechel et al., 2000; Merbold et al., 2009)), compiling



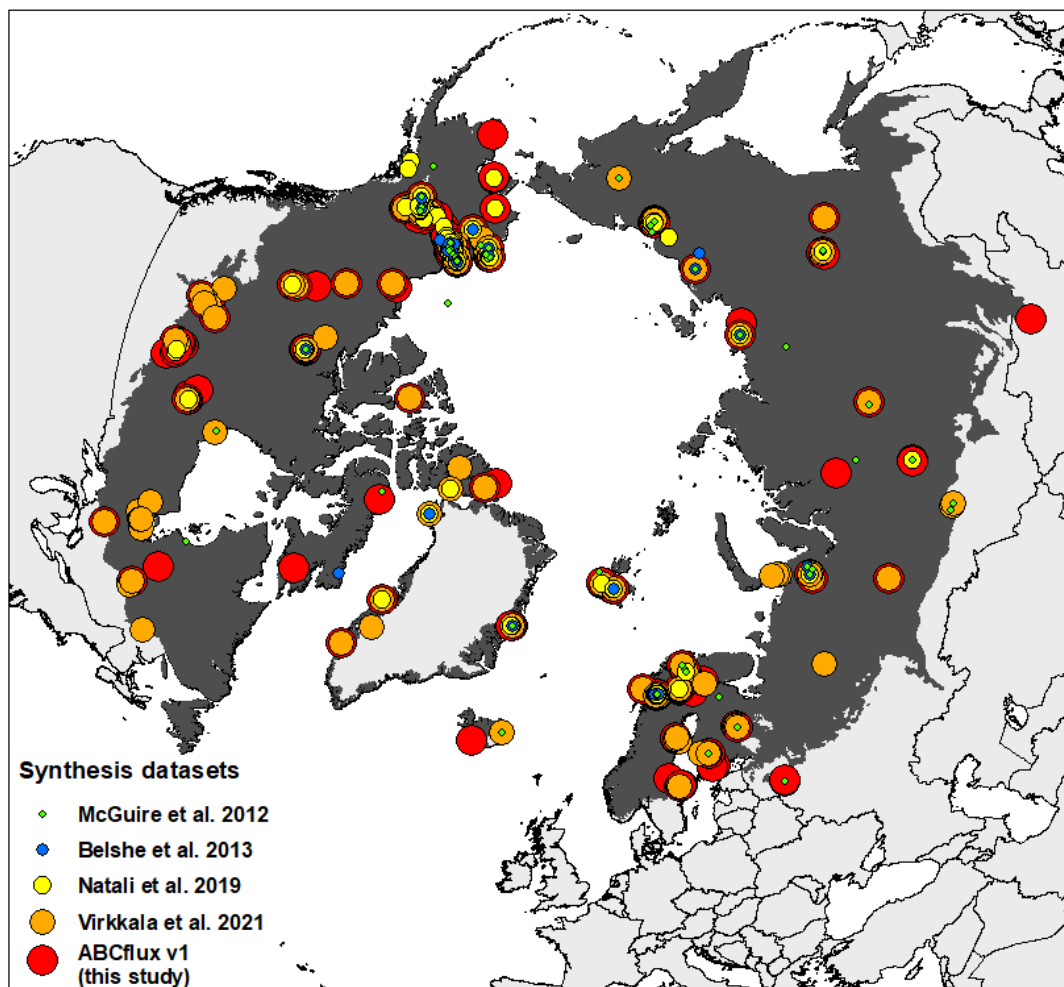
253 monthly fluxes has several advantages over the seasonal fluxes. These advantages include: (i)  
254 better comparability of measurements, (ii) ability to bypass problems related to defining seasons  
255 across large regions, and (iii) ease of linking these fluxes to remote sensing and models.

256

257 Our goal is to build upon past synthesis efforts and compile a new database of Arctic-Boreal CO<sub>2</sub>  
258 fluxes (ABCflux version 1) that combines eddy covariance, chamber, and diffusion data at  
259 monthly timescales with supporting environmental information to help facilitate large-scale  
260 assessments of the ABZ carbon cycle. This paper provides a general description of the ABCflux  
261 database by characterizing the data sources and database structure (Section 2), as well as  
262 describing the characteristics of the database (Section 3). Additionally, we describe the main  
263 strengths, limitations, and opportunities of this database (Section 4), and its potential utility for  
264 future studies aiming to understand terrestrial ABZ CO<sub>2</sub> fluxes.

265





266

267 **Fig 1.** The flux site distribution in previous syntheses that focused on compiling fluxes from high  
268 latitudes (McGuire et al. 2012, Belshe et al. 2013, Natali et al. 2019, Virkkala et al. 2021b and  
269 this study (ABCflux)). The Arctic-Boreal Zone is highlighted in dark grey; countries are shown  
270 in the background. Based on the unique latitude-longitude coordinate combinations in the tundra,  
271 there were 136 tundra sites in ABCflux, 104 tundra sites in Virkkala et al. 2021b, 68 tundra sites  
272 in Natali et al., 2019, 34 tundra sites in Belshe et al. 2013, and 66 tundra sites in McGuire et al.,  
273 2012. Observations that were included in previous studies but not in ABCflux represent fluxes  
274 aggregated over seasonal, not monthly periods.

275



276 **Table 1.** A summary of past CO<sub>2</sub> flux synthesis efforts. If site numbers were not provided in the  
 277 paper, this was calculated as the number of unique sets of coordinates.

Study	Number of sites	Synthesized fluxes and measurement techniques	Study domain	Study period	Flux aggregation
Luyssaert et al. (2007)	NA	GPP, Reco, and NEE measured with eddy covariance	Global forests (including boreal)	NA	Annual
McGuire et al. (2012)	60	GPP, Reco, and NEE measured with chambers, eddy covariance, diffusion technique and soda lime	Arctic tundra	Measurements from 1966-2009; focus on 1990-2009	Annual, growing and winter season
Belshe et al. (2013)	34	GPP, Reco, and NEE measured with chambers, eddy covariance, diffusion technique and soda lime	Arctic tundra	Measurements from 1966-2010	Annual, growing and winter season
Baldocchi et al. (2018)	9	GPP, Reco, and NEE measured with eddy covariance	Global (including boreal and tundra biomes)	NA (sites with 5-18 years of measurements)	Annual
Virkkala et al. (2018)	117	GPP, Reco, and NEE measured with chambers	Arctic tundra	Studies published during 2000-2016	Growing season
Natali et al. (2019)	104	Soil respiration (or NEE) measured with chambers, eddy covariance, diffusion	Northern permafrost region	Measurements from 1989-2017, focus on 2000-2017	Monthly or seasonal during winter



		technique, and soda lime			
Virkkala et al. (2021b)	148	GPP, Reco, and NEE measured with chambers and eddy covariance	Arctic tundra and boreal biomes	1990-2015	Annual and growing season
ABCflux version 1 (this study)	244	GPP, Reco, and NEE (with some soil respiration and forest floor fluxes) measured with chambers, eddy covariance, and diffusion technique	Arctic tundra and boreal biomes	1989-2020	Monthly (whole year)

278

## 279 2. Data and methods

280 ABCflux focuses on the area covered by the northern tundra and boreal biomes (>45 °N), as  
 281 characterized in (Dinerstein et al., 2017), Fig. 2)), and compiles *in-situ* measured terrestrial  
 282 ecosystem-level CO<sub>2</sub> fluxes aggregated to monthly time periods (unit: g C m<sup>-2</sup> month<sup>-1</sup>).

283 Although the three flux measurement techniques included in ABCflux primarily measure NEE,  
 284 chamber and eddy covariance techniques can also be used to estimate GPP (the photosynthetic  
 285 flux) and Reco (comprising emissions from autotrophic and heterotrophic respiration) (Keenan  
 286 and Williams, 2018), which are also included in the database. At eddy covariance sites, GPP and  
 287 Reco are indirectly derived from NEE using partitioning methods that primarily use light and  
 288 temperature data (Lasslop et al., 2010; Reichstein et al., 2005). At chamber sites, Reco can be  
 289 measured directly with dark chambers, from which GPP can be calculated by subtracting Reco  
 290 from NEE (Shaver et al., 2007). In general, these partitioned GPP and Reco fluxes have higher  
 291 uncertainties than the NEE measurements since they are modeled based on additional data and  
 292 various assumptions (Aubinet et al., 2012). However, GPP and Reco fluxes were included in

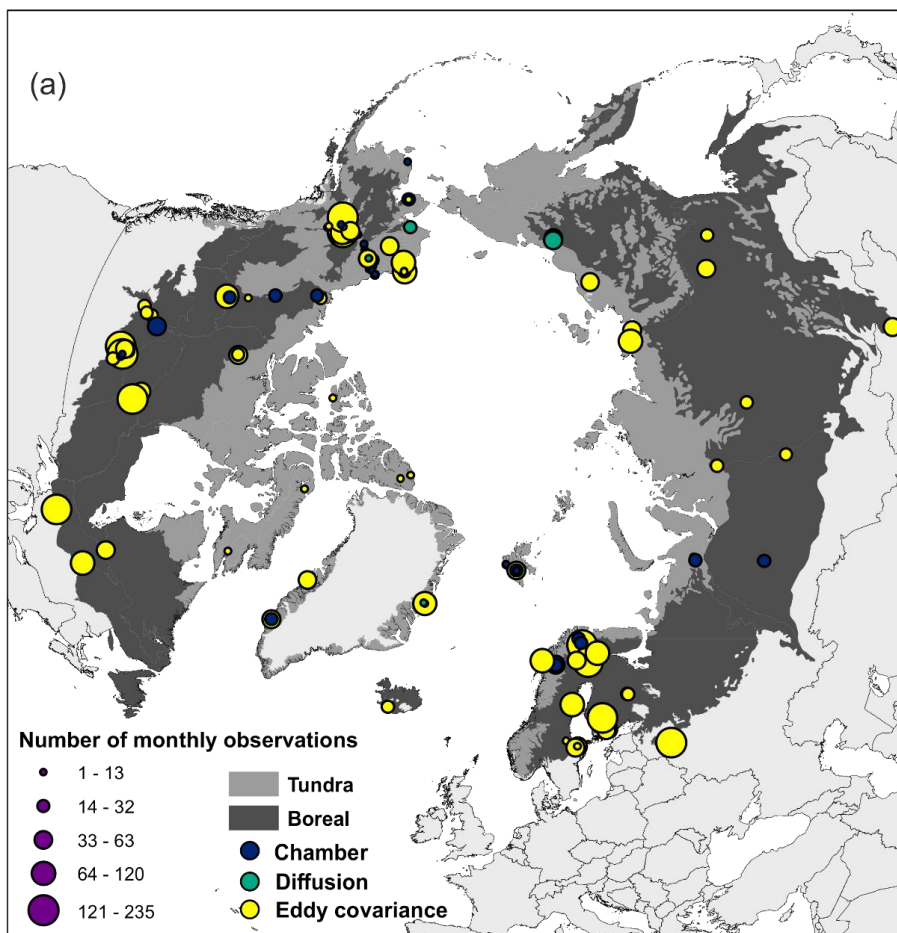


293 ABCflux because these component fluxes may help to better understand and quantify the  
294 underlying processes of land–atmosphere CO<sub>2</sub> exchange.

295

296 In addition to CO<sub>2</sub> fluxes, we gathered information describing the general site conditions (e.g.,  
297 site name, coordinates, vegetation type, disturbance history, a categorical soil moisture variable,  
298 and soil organic carbon stocks), micrometeorological and environmental measurements (e.g., air  
299 and soil temperatures, precipitation, soil moisture, snow depth), and flux measurement technique  
300 (e.g., measurement frequency, instrumentation, gap filling and partitioning method, number of  
301 spatial replicates for chamber measurements, flux data quality), wherever possible.

302





304 **Fig 2.** Map showing the distribution and measurement technique at each site (a), and examples of  
305 an eddy covariance tower (b), manual chamber (c), diffusion measurements (d), and two eddy  
306 covariance towers in wetland and forest (e). Photographs were taken in Yukon-Kuskokwim  
307 Delta, Alaska (September 2019), Kilpisjärvi, Finland (July 2016), Montmorency forest, Canada  
308 (April 2021), and Scotty Creek, Canada (April, 2014). Image credits to: Markus Jylhä, Alex  
309 Mavrovic, Gabriel Houde Gosselin, Chris Linder, Manuel Helbig.

310

311 2.1. Data sources

312 2.1.1 Literature search

313 We identified potential CO<sub>2</sub> flux studies and sites from prior synthesis efforts (Belshe et al.,  
314 2013; McGuire et al., 2012; Virkkala et al., 2018; Natali et al., 2019; Virkkala et al., 2021b),  
315 including a search of citations within and of the studies included in these prior syntheses. We  
316 also conducted a literature search with the search words (“carbon flux” or “carbon dioxide flux”  
317 or “NEE” or “net ecosystem exchange”), and (“arctic” or “tundra” or “boreal”) in Web of  
318 Science to ensure that our database included the most recent publications. We included studies  
319 that reported at least NEE, presented at monthly or finer temporal resolution, and had supporting  
320 environmental ancillary data describing the sites. We extracted our variables of interest (Section  
321 2.3.) from these selected papers during 2018-2020. Data from line and bar plots were extracted  
322 using Plot Digitizer (<http://plotdigitizer.sourceforge.net/>) and converted to our flux units (g C m<sup>-2</sup>  
323 month<sup>-1</sup>) if needed. Papers including a low number of temporal replicates within a month (<3  
324 individual measurements in summer months) and only one measurement month were  
325 disregarded. For the spring (March-May), autumn (September-November), and winter  
326 (December-February) months, one temporal replicate was accepted due to scarcity of  
327 measurements outside the summer season (June-August); measurement frequency is included in  
328 the database. Data from experimental treatments were excluded; however, we included flux data  
329 from unmanipulated control plots. Winter chamber or diffusion measurements in forests from  
330 Natali et al., (2019) were included in the “Ground\_NEE” field, which represents forest  
331 understory (not whole-ecosystem) NEE.

332



333 2.1.2. Flux repositories

334 We downloaded eddy covariance and supporting environmental data products from AmeriFlux  
335 (Novick et al., 2018), Fluxnet2015 (Pastorello et al., 2020), EuroFlux database cluster (ICOS,  
336 Carbon Extreme, Carbo Africa, GHG Europe, Carbo Italy, INGOS) (Paris et al., 2012; Valentini,  
337 2003), and Station for Measuring Ecosystem-Atmosphere Relations (Hari et al., 2013). Data  
338 were downloaded in 2018-2020. When only daily gap-filled data were supplied, we summed the  
339 data to monthly time steps and recorded the percentage of gap-filled data. We did not aggregate  
340 any repository GPP, Reco, or NEE datasets that were not gap filled. We filtered out  
341 measurements with low turbulence conditions based on friction velocity (USTAR) thresholds  
342 (Aubinet et al., 2012). USTAR varied among sites due to differing site-level assumptions. We  
343 downloaded only gap filled data that met the USTAR criteria for either the tower PI or given  
344 through the database processing pipeline. However, Fluxnet2015 provides several different  
345 methods for determining data quality based on different USTAR criteria. In this case, we used  
346 the Fluxnet2015 common USTAR threshold (CUT, i.e. all years at the site filtered with the same  
347 USTAR threshold (Pastorello et al., 2020)). For observations extracted from EuroFlux, USTAR  
348 thresholds for each site were derived as described in (Papale et al., 2006; Reichstein et al., 2005)  
349 using night-time data. If fluxes were available for the same period both in Natali et al., (2019)  
350 and flux repository extractions, the flux repository observations were kept in the database. Some  
351 repositories supplied eddy covariance data version numbers, which were added to the flux  
352 database.

353

354 2.1.3. Permafrost Carbon Network data solicitation

355 A community call was solicited in 2018 through a CO<sub>2</sub> flux synthesis workshop (Parmentier et  
356 al., 2019, Reconciling historical and contemporary trends in terrestrial carbon exchange of the  
357 northern permafrost-zone, 2021), whereby the network of ABZ flux researchers were contacted  
358 and invited to contribute their most current unpublished data. This resulted in an additional 39  
359 sites and 1372 monthly observations (see column `Extraction_source`).

360



361 2.2. Data quality screening

362 We screened for poor-quality data, potential unit and sign convention issues, and inaccurate  
363 coordinates. Repository data were processed and quality checked using quality flags associated  
364 with monthly data supplied by the repository processing pipeline. Fluxnet2015 and EuroFlux  
365 database include an aggregated data quality flag (fraction between 0-1, indicating percentage of  
366 measured and good-quality gap-filled data; average from daily data; 0=extensive gap-filling,  
367 1=low gap-filling; for more details see (Pastorello et al., 2020)) which is reported for fluxes  
368 aggregated from finer temporal resolutions. We removed monthly data with a quality flag of 0.  
369 Eddy covariance data with quality flags >0 were left within the database for the user to decide on  
370 additional screening criteria. The database also includes a column describing the percentage of  
371 gap-filled data (0=no gap-filled data, 100=completely gap-filled data), however it was not used  
372 in data quality screening. These fields describe the amount and quality of the gap-filled data that  
373 need to be filled due to, for example, instrument malfunction, power shortage, extreme weather  
374 events, and periods with insufficient turbulence conditions.

375

376 We further screened for spatial coordinate accuracy by visualizing the sites on a map. If a given  
377 site was located in water or had imprecise coordinates, the site researchers were contacted for  
378 more precise coordinates. We screened for potential duplicate sites and observations that were  
379 extracted from different data sources. Duplicate NEE extracted from papers that were also  
380 extracted from flux repositories were compared to estimate uncertainties associated with using  
381 Plot Digitizer as a means for extracting monthly fluxes. A linear regression between paper (Plot  
382 Digitizer) and repository extraction showed that data extracted using Plot Digitizer were highly  
383 correlated with data from online databases, providing confidence in estimates extracted using  
384 Plot Digitizer ( $R^2=0.91$ , slope = 1.002,  $n=192$ ). Out of these duplicate observations, we only kept  
385 the data extracted from the repository in the database. Finally, we asked site principal  
386 investigators (PIs) to verify that the resulting information was correct.

387

388 2.3. Database structure and columns

389 The resulting ABCflux database includes 94 variables: 16 are flux measurements and associated  
390 metadata (e.g., NEE, measurement date and duration), 21 describe flux measurement methods





391 (e.g., measurement frequency, gap-filling method), 49 describe site conditions (e.g., soil  
 392 moisture, air temperature, vegetation type), and 8 describe the extraction source (e.g., primary  
 393 author or site PI, citation, data maturity). 61 variables are considered static and thus do not vary  
 394 with repeated measurements at a site (e.g., site name, coordinates, vegetation type), while 33  
 395 variables are considered dynamic and vary monthly (e.g., soil temperature). Table 2 includes a  
 396 description of each of the 94 variables, as well as the proportion of monthly observations present  
 397 in each column. ABCflux is shared as a comma separated values (csv) file with 6309 rows;  
 398 however, not all the rows have data in each column (indicated by NA).

399

400 We refer to all fields included in ABCflux as observations although we acknowledge that, for  
 401 example, GPP and Reco are indirectly derived variables at eddy covariance sites, and that some  
 402 flux and ancillary data can also be partly gap-filled. Further, our database does not include the  
 403 actual raw observations, rather it provides monthly aggregates. Positive values for NEE indicate  
 404 net CO<sub>2</sub> loss to the atmosphere (i.e., CO<sub>2</sub> source) and negative numbers indicate net CO<sub>2</sub> uptake  
 405 by the ecosystem (i.e., CO<sub>2</sub> sink). For consistency, GPP is presented as negative (uptake) values  
 406 and Reco as positive.

407

408 **Table 2.** Database variables and the proportion of monthly observations in each variable. There  
 409 are in total 6309 monthly observations in the database.

410

Variable	Variable description and units	Details	Proportion of monthly observations having data
id	ID given to each individual monthly entry at each site		100%
Study_ID	ID given to study/site entry (see Details)	(PI/first author of publication)_(site name)_(tower/chamber)_(#); Eg., Schuur_EML_Tower_1. Note that there might be several chamber (or tower) Study_IDs for one site.	100%



Study_ID_Short	ID given to study/site entry (see Details), individual chamber plots within a site not differentiated	(PI/first author of publication)_(site name)_(tower/chamber)_(#); Eg., Schuur_EML_Tower_1.	100%
Site_Name	Site name as specified in data source	Usually the location name	100%
Site_Reference	A more specific name used in data source	For towers, this is often the acronym for the site, and for chambers, this is the name of the particular chamber plot	95%
Data_contributor_or_Author	Data contributor(s) or primary author(s) associated with data set or publication	If you use unpublished data or data from flux repositories (see Extraction_source), please contact this person	100%
Latitude	Decimal degrees, as precise as possible		100%
Longitude	Decimal degrees, as precise as possible	Negative longitudes are west from Greenwich	100%
Email	Primary author email		93%
ORCID	personal digital identifier: <a href="https://orcid.org/">https://orcid.org/</a>		29%
Citation	Journal article, data citation, and/or other source (online repository, PI submitted, etc.).		70%
Data_adder	The person(s) who added the data to the database	Primarily researchers working at Woodwell	100%
Data_availability	Current availability of data: data available in a published paper, in an open online data repository, in an already published synthesis, or user contributed	Published_Paper, Published_Online, Published_Synthesis, User_Contributed	100%
Data_maturity	Current maturity of data	Preliminary, Processed, Published, Reprocessed	100%



Extraction_source	Data source	paper, Virkkala or Natali syntheses, Euroflux, Fluxnet 2015, PI, Ameriflux, SMEAR, ORNL DAAC, Pangaea	100%
Biome	Biome of the site	Boreal, Tundra	100%
Veg_type	A detailed vegetation type for the site	B1=cryptogram, herb barren; B2=cryptogram barren complex; B3=noncarbonate mountain complex; B4=carbonatemountain complex; G1=rush/grass, forb, cryptogram tundra; G2=graminoid, prostrate dwarf-shrub, forb tundra; G3=nontussock sedge, dwarf-shrub, moss tundra; G4=tussock-sedge, dwarf-shrub, herb tundra; P1=prostrate dwarf-shrub, herb tundra; P2=prostrate/hemiprostrate dwarf-shrub tundra; S1=erect dwarf-shrub tundra; S2=low-shrub tundra; W1=sedge/grass, moss wetland; W2=sedge, moss, dwarf-shrub wetland; W3=sedge, moss, low-shrub wetland; DB=deciduous broadleaf forest; EN=evergreen needleleaf forest; DN=deciduous needleleaf forest; MF=mixed forest; SB=sparse boreal vegetation; BW=boreal wetland or peatland, following Watts et al. (2019). For more details about the tundra vegetation types, see Walker et al. (2005). These classes were classified based on information in Site_Reference and Veg_detail columns, or were contributed by the site PI.	100%
Veg_type_Short	A more general vegetation type for the site	B=barren tundra; G=graminoid tundra; P=prostrate dwarf-shrub tundra; S=shrub tundra; W=tundra wetland; DB=deciduous broadleaf forest; EN=evergreen needleleaf forest; DN=deciduous needleleaf forest; MF=mixed forest; SB=sparse boreal vegetation; BW=boreal wetland or peatland. For more details about the tundra vegetation types, see Walker et al. (2005). These classes were classified based on information in Site_Reference and Veg_detail columns, or were contributed by the site PI.	100%
Veg_detail	Detailed vegetation description from data source/contributor		96%
Country	Country of the site		100%
Permafrost	Reported presence or absence of permafrost	Yes, No	72%



Disturbance	Last disturbance	Fire, Harvest, Thermokarst, Drainage, Grazing, Larval Outbreak, Drought	30%
Disturb_year	Year of last disturbance	Numeric variable, 0 = annual (e.g., annual grazing)	23%
Disturb_severity	Relative severity of disturbance	High, Low	11%
Soil_moisture_class	General descriptor of site moisture	Wet = At least sometimes inundated or water table close to surface. Dry = well-drained.	56%
Site_activity	Describes whether the site is currently active (i.e., measurements conducted each year)	Yes, No. Eddy covariance information was extracted from <a href="https://cosima.nceas.ucsb.edu/carbon-flux-sites/">https://cosima.nceas.ucsb.edu/carbon-flux-sites/</a> by assuming that sites that were active in 2017 are still continuing to be active. We used our expertise to define active chamber sites that have measurements at least during each growing season.	60%
Meas_year	Year in which data were recorded		100%
Season	Season in which data were recorded	summer, autumn, winter, spring (based on climatological seasons)	100%
Interval	Measurement month		100%
Start_day	Start day of the measurement		100%
End_day	End day of the measurement		100%
Duration	Number of days during the measurement month	Should be the same as End_Day because this database compiles monthly fluxes	100%
Start_date	Date on which measurement starts	dd/mm/yyyy	100%
End_date	Date on which measurement ends	dd/mm/yyyy	100%
NEE_gC_m2	Net Ecosystem Exchange (g C-CO <sub>2</sub> m <sup>-2</sup> for the entire measurement interval)	Convention: -ve is uptake, +ve is loss.	91%



GPP_gC_m2	Gross Primary Productivity (g C-CO <sub>2</sub> m <sup>-2</sup> for the entire measurement interval)	Report as -ve flux	68%
Reco_gC_m2	Ecosystem Respiration (g C-CO <sub>2</sub> m <sup>-2</sup> for the entire measurement interval)	Report as +ve flux	73%
Ground_NEE_gC_m2	Forest floor Net Ecosystem Exchange, measured with chambers (g C-CO <sub>2</sub> m <sup>-2</sup> for the entire measurement interval)	Convention: -ve is uptake, +ve is loss. Chamber measurements from (primarily rather treeless) wetlands are included in the NEE_gC_m2 column.	4%
Ground_GPP_gC_m2	Forest floor Ecosystem Respiration, measured with chambers (g C-CO <sub>2</sub> m <sup>-2</sup> for the entire measurement interval)	Report as -ve flux. Chamber measurements from (primarily rather treeless) wetlands are included in the GPP_gC_m2 column.	1%
Ground_Reco_gC_m2	Forest floor Gross Primary Productivity, measured with chambers (g C-CO <sub>2</sub> m <sup>-2</sup> for the entire measurement interval)	Report as +ve flux. Chamber measurements from (primarily rather treeless) wetlands are included in the Reco_gC_m2 column.	2%
Rsoil_gC_m2	Soil respiration, measured with chambers (g C-CO <sub>2</sub> m <sup>-2</sup> for the entire measurement interval)	Report as +ve flux	4%
Flux_method	How flux values were measured	EC=eddy covariance, Ch=chamber, Diff=diffusion methods. No observations from experimental manipulation plots	100%
Flux_method_detail	Details related to how flux values were measured: closed- and open-path eddy covariance, mostly manual chamber measurements, mostly automated chamber measurements, a combination of chamber and cuvette measurements, diffusion measurements through the snowpack, chamber measurements on top of snow	EC_closed, EC_open, EC_enclosed, EC_open & closed, EC_enclosed, Chambers_mostly_manual, Chambers_mostly_automatic, Chambers_CUV, Snow_diffusion, Chambers_snow, NA	93%



Measurement_frequency	Frequency of flux measurements	>100 characterizes high-frequency measurements. Manual chamber and diffusion techniques often have values between 1 and 30; 1=measurements done during one day of the month, 30=measurements done daily throughout the month.	100%
Diurnal_coverage	Times of day covered by flux measurements	Day, Day and Night	90%
Partition_method	Method used to partition NEE into GPP and Reco	Reichstein (night time=Reco partitioning), Lasslop (bulk/day-time partitioning), Reco_measured, ANN, or GPP=Reco-NEE (for chamber sites)	16%
Spatial_reps_chamber	Number of spatial replicates for the chamber plot	Usually, but not always, several chamber plots are measured to assure the representativeness of measurements	71%
Gap_fill	Gap filling method	e.g., Average, Linear interpolation, Lookup table, MDS (marginal distribution sampling), Light/temperature response, Neural network, a combination of these, or a longer description related to chamber measurements	70%
Gap_perc	% of NEE data that was gap-filled in the measurement interval (relative to standard measurement time step)		17%
Tower_QA.QC.NEE.flag	Overall monthly quality flag for eddy covariance aggregated observations; fraction between 0-1, indicating percentage of measured and good-quality gap-filled data	0=extensive gap-filling, 1=low gap-filling	44%
QA.QC.source	The source for the overall quality information for the eddy covariance observations	0=Fluxnet2015, 1=Euroflux	37%
Precip_int_mm	Total precipitation during measurement interval (mm)		37%
Tair_int_C	Mean air temperature during measurement interval (°C)		72%



Tsoil_C	Mean soil Temperature during measurement interval (°C)		74%
Soil_moisture_perc	Mean soil moisture during the measurement interval (% by volume)		35%
Thaw_depth_cm	Mean thaw depth during the measurement interval (cm)	Report with positive values	6%
Tsoil_depth_cm	Depth of soil temperature measurement below surface (cm)		46%
Moisture_depth_cm	Depth of soil moisture measurement below surface (cm)		31%
ALT_cm	Active layer thickness (cm; maximum thaw depth), will change annually	Report with positive values	15%
WTD_cm	Mean water table depth during the measurement interval (cm); Positive is below the surface, negative is above (inundated)		7%
Snow_depth_cm	Mean snow depth during the measurement interval (cm)		14%
VPD_Pa	Mean vapour pressure deficit during the measurement interval (Pa)		30%
ET_mm	Total evapotranspiration during the measurement interval (mm)		4%
PAR_W_m2	Mean photosynthetically active radiation during measurement interval ( $W m^{-2}$ )		5%



PAR_PPFD_umol_m2_s	Mean photosynthetically active radiation during measurement interval (measured in Photosynthetic Photon Flux Density, PPFD; micromol m <sup>-2</sup> s <sup>-1</sup> )		11%
Precip_ann_mm	Mean annual precipitation (mm), from site or nearby weather station as a general site descriptor. This should describe the longer-term climate for the site rather than a few years of study.		80%
Tair_ann_C	Mean annual air temperature (°C), from site or nearby weather station as a general site descriptor. This should describe the longer-term climate for the site rather than a few years of study.		79%
Met_source	Data source and years used to calculate mean annual temperature/precipitation		50%
Elevation_m	Elevation above sea level (m)		65%
LAI	Leaf Area Index		23%
SOL_depth_cm	Soil organic layer depth (cm)		23%
perc_C	Soil carbon percentage (%)		7%
perc_C_depth_cm	Depth at which soil carbon % was measured (cm)		7%
C_dens_kgC_m2	Soil carbon per unit area (kg C m <sup>-2</sup> )		16%
C_dens_depth_cm	Depth to which Soil organic carbon per unit area was		8%





	estimated (cm)		
AGB_kgC_m2	Above ground biomass (kg C m <sup>-2</sup> )		11%
AGB_type	Types of above ground vegetation included in the AGB measurement	Trees, shrubs, graminoids, mosses, lichens	13%
Soil_type	General soil type, including source (e.g., USDA, CSSC, NCSCD)		42%
Soil_type_detail	Detailed soil type description, if available		9%
Citation_Data_Overlap	Another citation for the site		13%
High_freq_availability	Availability of high-frequency data		17%
Light_response_method_chamber	Details related to how the varying light response conditions were considered in chamber measurements		5%
PAR_cutoff_umol_m2_second	PAR level used to define nighttime data and apply partitioning method (umol PAR m <sup>-2</sup> second <sup>-1</sup> )		17%
Aggregation_method	Method used to aggregate data to measurement interval		58%
Instrumentation	Description of instrumentation used		68%
Tower_Version	Version number of the eddy covariance dataset from the extraction source		21%
Spatial_variation_technique	Technique used to quantify spatial variation for flux measurements	e.g., standard error of replicate measurements for chambers, spatial error based on footprint partitioning for towers	10%



Method_error_NEE_gC_m 2	RMSE or other bootstrapped error of model fit for NEE (g C-CO <sub>2</sub> m <sup>-2</sup> for the entire measurement interval)		23%
Method_error_technique	Technique used to quantify method errors for flux measurements	e.g., gap-filling and partitioning errors or uncertainty in data-model fit: bootstrap, MCMC, RMSE fit, etc.	1%
Tower_Data_restriction			12%
Tower_Corrections	Details related to processing corrections employed, including time, duration, and thresholds for u* and heat corrections		32%
Other_data	Other types of data from the data source that may be relevant		7%
Notes_SiteInfo	Any other relevant information		20%
Notes_TimeVariant	Any other relevant information		59%

411

412

413

#### 414 2.4. Database visualization

415 The visualizations in this paper were made with the full ABCflux database using each site-month  
 416 as a unique data point (from now on, these are referred to as monthly observations) and the sites  
 417 listed in the “Study\_ID\_Short” field. We visualized these across the vegetation types  
 418 (“Veg\_type\_Short”), countries (“Country”), biomes (“Biome”), and measurement method  
 419 (“Flux\_method”).

420

421 To understand the distribution and representativeness of monthly observations and sites across  
 422 the ABCflux as well as the entire ABZ, we used geospatial data to calculate the aerial coverages  
 423 of each vegetation type and country. Vegetation type was derived from the European Space  
 424 Agency Climate Change Initiative’s (ESA CCI) land cover product aggregated and resampled to



425 0.0083° for the boreal biome (Lamarche et al., 2013) and the raster version of the Circumpolar  
426 Arctic Vegetation Map (CAVM) for the tundra biome resampled to the same resolution as the  
427 ESA CCI product (Raynolds et al., 2019). ESA CCI layers were reclassified by grouping land  
428 cover types to the same vegetation type classes represented by ABCflux: boreal wetland and  
429 peatland (from now on, boreal wetland; classes 160, 170, 180 in ESA CCI product), deciduous  
430 broadleaf forest (60-62), evergreen needleleaf forest (70-72), deciduous needleleaf forest (80-  
431 82), mixed forest (90), and sparse and mosaic boreal vegetation (40, 100, 100, 120, 121, 122,  
432 130, 140, 150, 151, 152, 153, 200, 201, 202). Croplands (10, 11, 12, 20, 30) and urban areas  
433 (190) were removed. We used the five main physiognomic classes from CAVM in the tundra.  
434 Glaciers and permanent water bodies included in either of these products were removed. Note  
435 that in ABCflux and for the site-level visualizations in this paper, vegetation type for each of the  
436 flux sites was derived from site-level information, not these geospatial layers. These same  
437 glacier, water, and cropland masks were applied to the country boundaries (Natural Earth - Free  
438 vector and raster map data at 1:10m, 1:50m, and 1:110m scales, 2021) to calculate the terrestrial  
439 area of each country.

440

### 441 3. Database summary

#### 442 3.1. General characteristics of the database

443 ABCflux includes 244 sites and 6309 monthly observations, out of which 136 sites and 2217  
444 monthly observations are located in the tundra (54 % of sites and 52 % of observations from  
445 North America, 46 % and 48 % from Eurasia), while 108 sites and 4092 monthly observations  
446 are located in the boreal biome (59 % of sites and 58 % of observations from North America, 41  
447 % and 42 % from Eurasia) (Table 3). The largest source of flux data are the flux repositories (48  
448 % of the monthly observations), while flux data extracted from papers or contributed by site PIs  
449 amount to 30 % and 22 % of the monthly observations, respectively. The database primarily  
450 includes sites in unmanaged ecosystems, but it does contain a small number (6) of sites in  
451 managed forests.

452



453 **Table 3.** General statistics of the database. Number of monthly CO<sub>2</sub> flux measurements and sites  
 454 derived from eddy covariance, chamber, and diffusion techniques, and the proportion of data  
 455 coming from different data sources. Note that some of the data extracted from flux repositories  
 456 and papers were further edited by the PIs; this information can be found in the database. For this  
 457 table, observations that were fully contributed by the PI were considered as PI-contributed.  
 458

Flux measurement technique	Number of sites	Number of observations	Number of observations derived using different eddy covariance and chamber techniques	Number of observations extracted from different data sources
Eddy covariance	Total: 119 Tundra: 47 Boreal: 72	Total: 4957 Tundra: 1406 Boreal: 3551	Open-path: 1988 Closed path: 2085 Both: 245 Enclosed: 240 No information available: 399	Flux repository: 2775 Published: 810 PI-contributed: 1350
Chamber	Total: 104 Tundra: 73 Boreal: 31	Total: 1166 Tundra: 708 Boreal: 458	Manual: 435 Automated: 696 No information available: 35	Flux repository: 243 Published: 901 PI-contributed: 22
Diffusion	Total: 21 Tundra: 16 Boreal: 5	Total: 186 Tundra: 103 Boreal: 83		Flux repository: 0 Published: 186 PI-contributed: 0

459  
 460  
 461 The majority of observations in ABCflux have been measured with the eddy covariance  
 462 technique (119 sites and 4957 monthly observations), whereas chambers and diffusion methods  
 463 were used at 125 sites and 1352 observations (Table 3). About 46 % of the eddy covariance  
 464 measurements are based on gas analyzers using closed-path technology (including enclosed  
 465 analyzers), 40 % are based on open-path technology, 5 % include both and 8 % are unknown. 52  
 466 % of chamber measurements were automated chambers (monitoring the fluxes continuously  
 467 throughout the growing season). Only 3 % of the measurements were completed using diffusion  
 468 methods during the winter. Chamber and diffusion studies were primarily from the tundra and  
 469 the sparsely treed boreal wetlands, but a few studies with ground surface CO<sub>2</sub> fluxes from forests

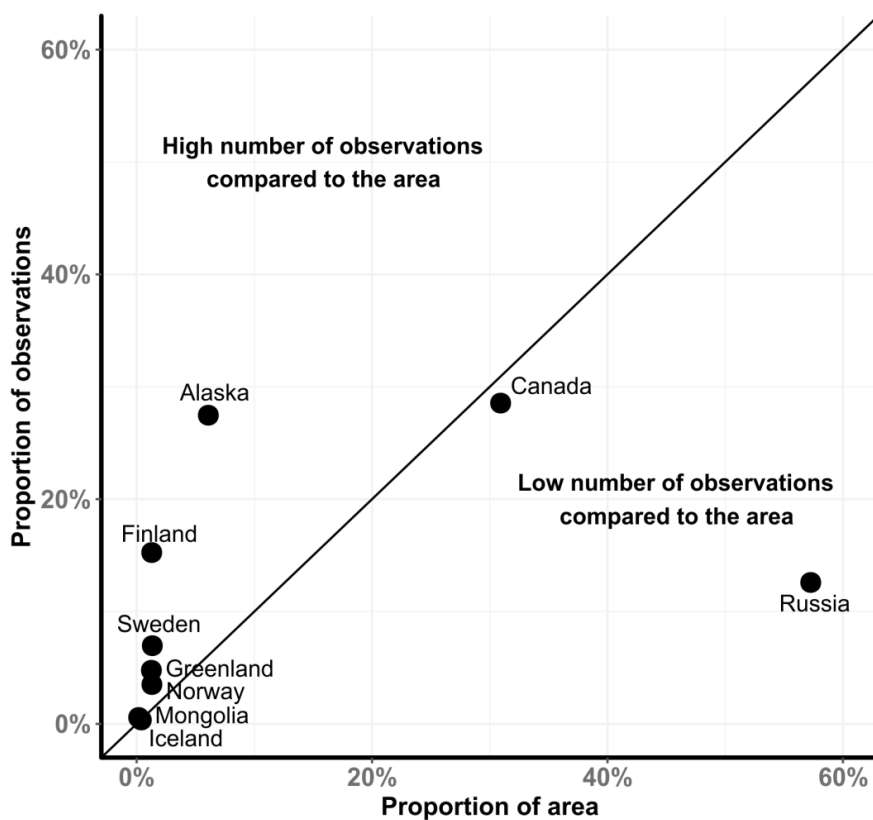


470 (i.e., capturing the ground cover vegetation and not the whole ecosystem) are also included in  
471 their own fields so that they can not be mixed up with ecosystem-scale measurements  
472 (“Ground\_NEE\_gC\_m2”, ”Ground\_GPP\_gC\_m2”, “Ground\_Reco\_gC\_m2”). Further, a few soil  
473 CO<sub>2</sub> flux sites measuring fluxes primarily on unvegetated surfaces during the non-growing  
474 season are included in the database (“Rsoil\_gC\_m2”). These were included in the database  
475 because ground surface or soil fluxes during the non-growing season can be of similar magnitude  
476 to the ecosystem-level fluxes when trees remain dormant (Ryan et al., 1997; Hermle et al., 2010).  
477 Therefore, these ground or soil fluxes could potentially be used to represent ecosystem-level  
478 fluxes during some of the non-growing season months. However, we did not make an extensive  
479 literature search for these observations, rather we compiled observations if they came up in our  
480 NEE search. Therefore, the data in these ground surface and soil flux columns represents only a  
481 portion of such available data across the ABZ.

482

483 The geographical coverage of the flux data is highly variable across the ABZ, with most of the  
484 sites and monthly observations coming from Alaska (37 % of the sites and 28 % of the monthly  
485 observations), Canada (19 % and 29 %), Finland (7 % and 15 %), and Russia (14 % and 13 %)  
486 (Fig. 3). The sites cover a broad range of vegetation types, but were most frequently measured in  
487 evergreen needleleaf forests (23 % of the sites and 37 % of the monthly observations) and  
488 wetlands in the tundra or boreal zone (30 % and 27 %) (Fig. 4). The northernmost and  
489 southernmost ecosystems had fewer sites and observations than more central ecosystems (barren  
490 tundra: 45% of the sites and 3 % of the monthly observations, prostrate shrub: 2 % and <1 %,  
491 deciduous broadleaf forest: 1 % and 3 %, deciduous needleleaf forest: 5 % and 4 %, mixed forest  
492 <1 % and <1 %). ABCflux includes sites experiencing various types of disturbances, with the  
493 majority of disturbed sites encountering fires (24 sites and 901 monthly observations),  
494 thermokarst (4 sites and 113 monthly observations), or harvesting (6 sites and 258 monthly  
495 observations). However, ABCflux is dominated by sites in relatively undisturbed environments  
496 or sites lacking disturbance information (only 20 % of the sites and 30 % of the monthly  
497 observations include disturbance information).

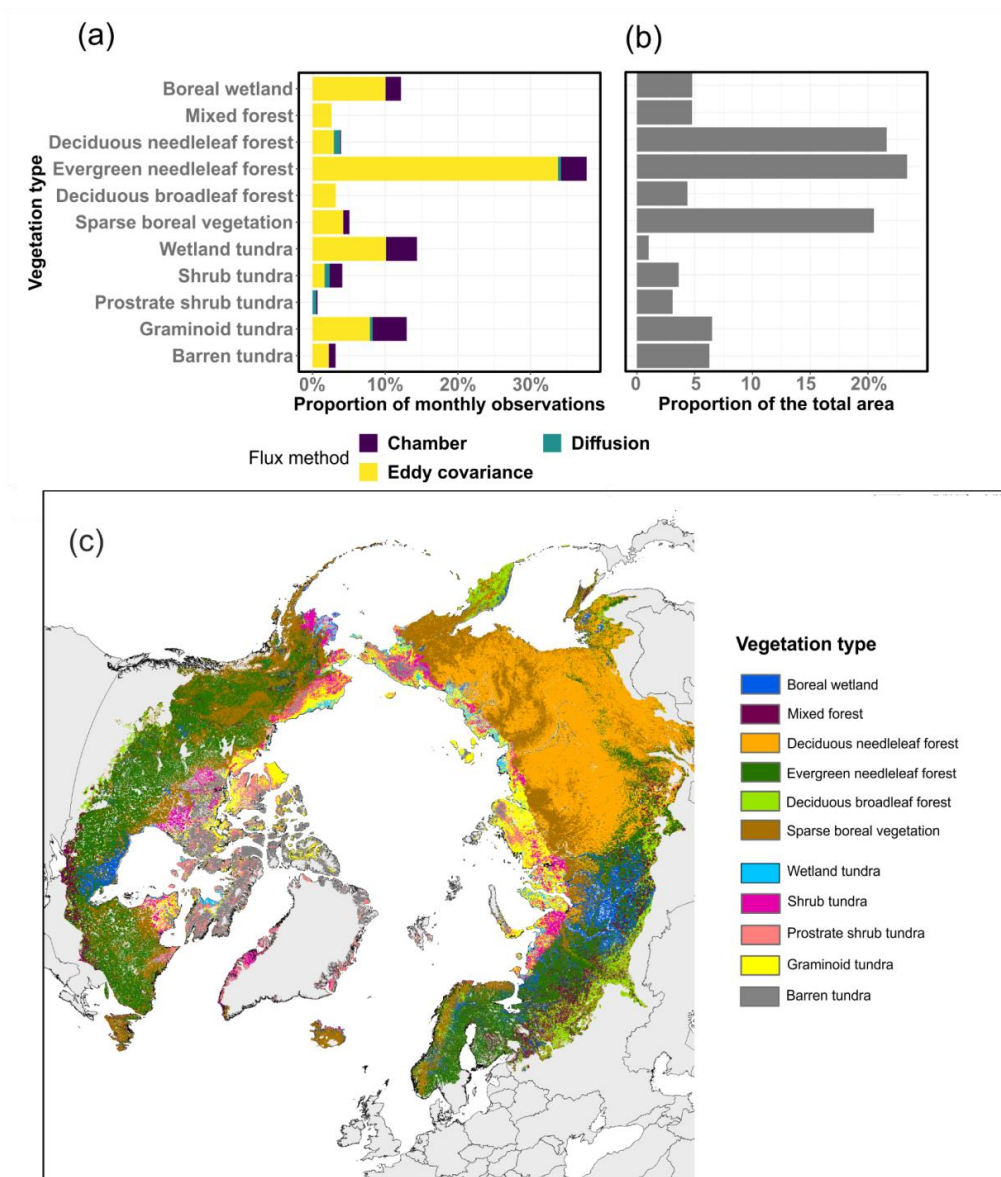
498



499

500 **Fig 3.** The proportion of monthly observations in each country/region compared to the  
501 proportion of the areal extent of the country/region across the entire Arctic-Boreal Zone. Ideally,  
502 points would be close to the 1:1 line (i.e., large countries/regions have more observations than  
503 small countries/regions). Permanent water bodies, croplands, and urban areas were masked from  
504 the areal extent calculation.

505



506

507



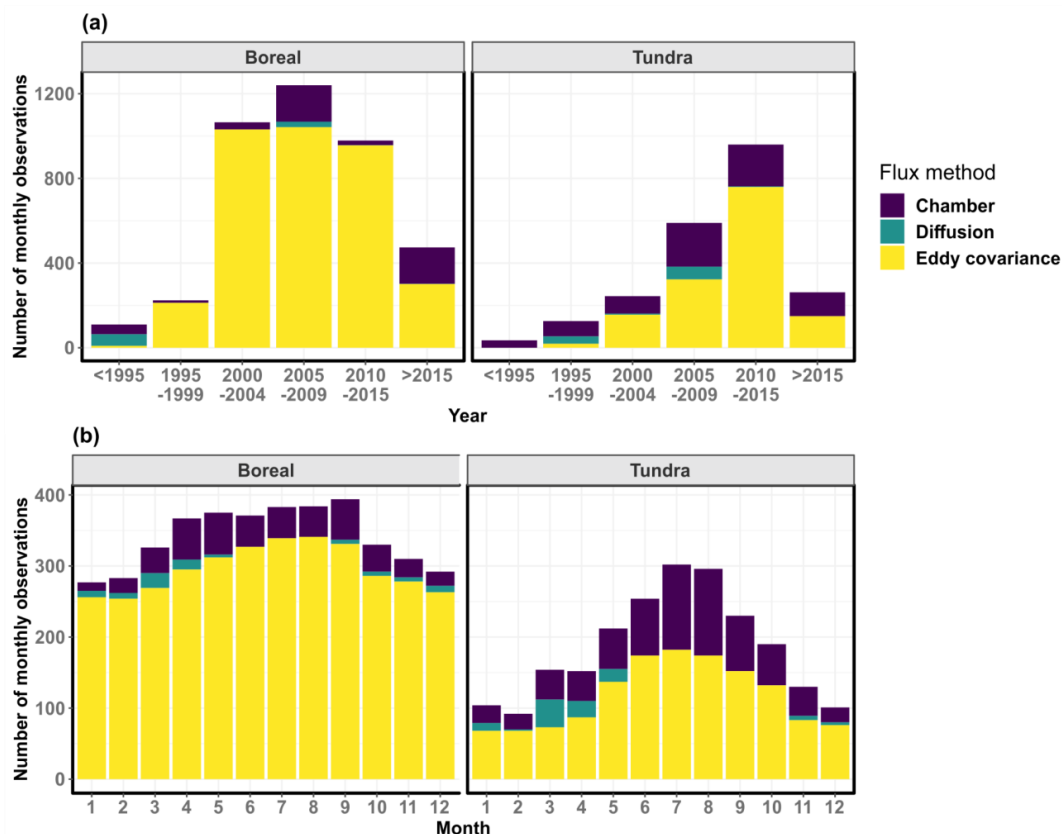
508 **Fig 4.** The proportion of monthly observations in each vegetation type colored by the flux  
509 measurement technique (a) and the proportion of the areal extent of each vegetation type across  
510 the entire Arctic-Boreal Zone (b). Permanent water bodies, croplands, and urban areas were  
511 masked from the areal extent calculation. Sparse boreal vegetation class in the vegetation map  
512 includes vegetation mixtures and mosaics.

513

514 ABCflux spans a total of 31 years (1989-2020), but the largest number of monthly observations  
515 originate from 2000-2015 (80 % of the data) (Fig. 5). The largest number of measurements were  
516 conducted during the summer (June-August; 32 %) and the least during the winter (November-  
517 February; 18 %) (Fig. 5). The overall eddy covariance data quality and gap-filled data percentage  
518 were lowest during the winter compared to other seasons (0.76 compared to 0.8-0.85 for overall  
519 data quality, 0=extensive gap-filling, 1=low gap-filling; 69 % compared to 47 to 59 % for gap-  
520 filled data percentage).

521





522

523 **Fig 5.** Histograms showing the number of monthly measurements across five-year periods (a)  
524 and across the tundra and boreal biomes (b). The bar plots are colored by the flux measurement  
525 technique. Chambers in the boreal biome measured fluxes in treeless or sparsely treed areas  
526 (primarily wetlands).

527

### 528 3.2. Coverage of ancillary data

529

530 All of the observations in ABCflux include information describing the site name, location,  
531 vegetation type, NEE, measurement technique (eddy covariance/chamber/diffusion), and how the  
532 data were compiled (Table 2). Details about the measurement technique (e.g., open or closed-  
533 path eddy covariance, manual or automated chambers) are included in 93 % of sites and 93 % of  
534 monthly observations. Most of the monthly observations further include information about



535 permafrost extent ( 67 % of the sites and 72 % of the monthly observations), or soil moisture  
536 state (47 % of the sites and 56 % of the monthly observations). Data describing air temperature,  
537 soil temperature, precipitation, and soil moisture are included in 71, 73, 37, and 35 % of monthly  
538 observations, respectively. Some ancillary variables have low data coverage, such as soil organic  
539 carbon stocks (16 % of the monthly observations) or active layer thickness (15 % of the monthly  
540 observations).

541

### 542 3.3. Coverage and distribution of flux data

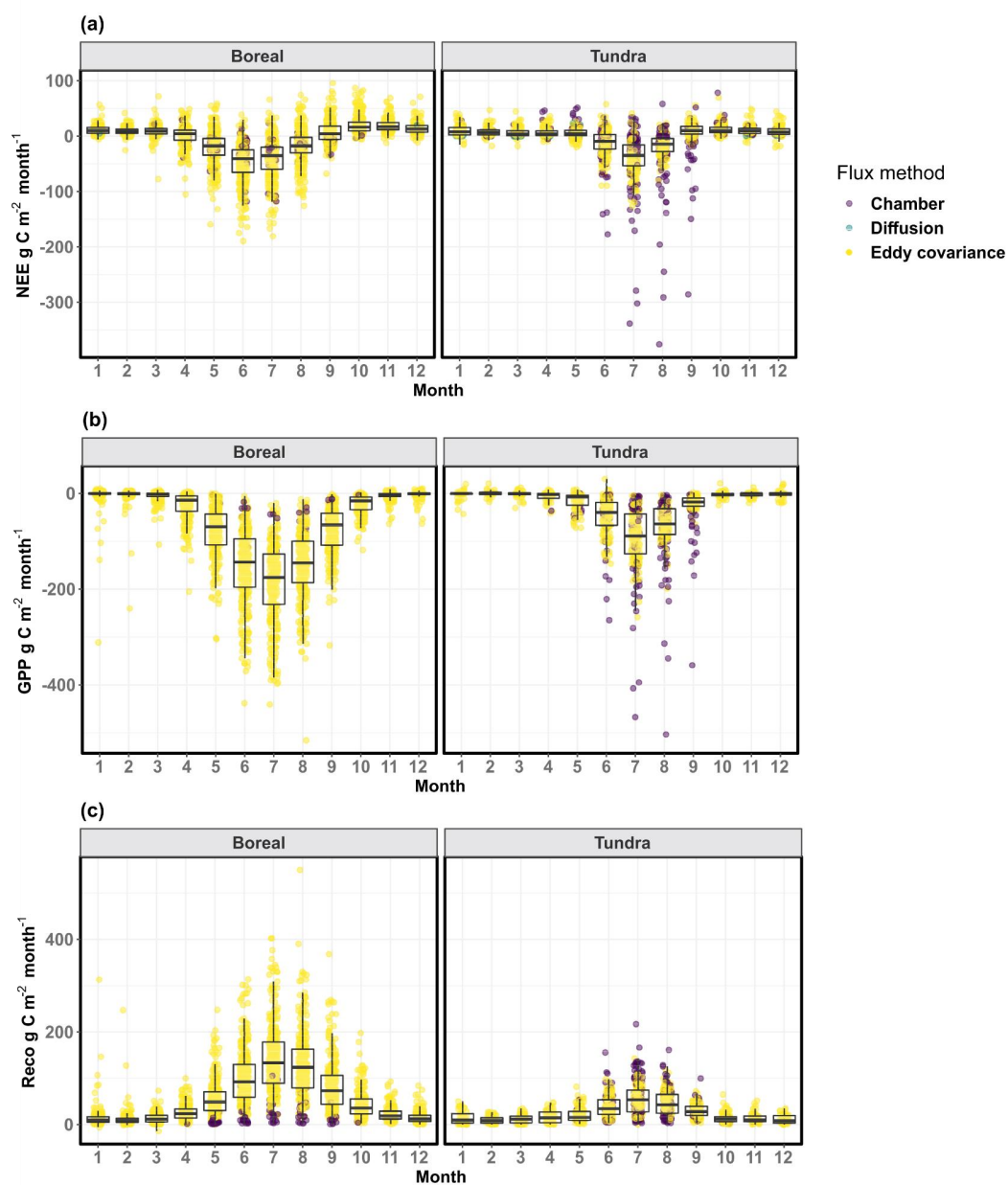
543

544 There are 110 sites and 4290 monthly observations for GPP, 121 sites and 4603 monthly  
545 observations for Reco, and 212 sites and 5759 monthly observations for NEE in ABCflux.  
546 Monthly values range from -2 to -516 g C m<sup>-2</sup> month<sup>-1</sup> for GPP, from 0 to 550 g C m<sup>-2</sup> month<sup>-1</sup>  
547 for Reco, and from -376 to 95 g C m<sup>-2</sup> month<sup>-1</sup> for NEE (Table 4). NEE is typically negative  
548 during the summer (i.e., net CO<sub>2</sub> sink) and mostly positive during other seasons (i.e., net CO<sub>2</sub>  
549 source) (Fig. 6). Out of all site and year combinations, annual cumulative NEE (the sum of  
550 monthly NEE values for each year and site) can be calculated for 267 site-years. An average  
551 annual NEE calculated based on the site-level averages from 1995 to 2020 is -27.9 g C m<sup>-2</sup> year<sup>-1</sup>  
552 (SD 85.4) for the entire region, -35.5 g C m<sup>-2</sup> year<sup>-1</sup> (SD 93.7) for the boreal biome, and -3.3 g C  
553 m<sup>-2</sup> year<sup>-1</sup> (SD 44.2) for the tundra. However, these averages do not account for the spatial or  
554 temporal distribution of the observations, and therefore represent coarse summaries of the  
555 database.

556

557

558



559

560 **Fig 6.** The distribution of net ecosystem exchange (NEE; a), gross primary productivity (GPP;  
561 b), and ecosystem respiration (Reco; c) across the months, colored by the flux measurement  
562 technique. Positive numbers for NEE indicate net CO<sub>2</sub> loss to the atmosphere (i.e., CO<sub>2</sub> source)  
563 and negative numbers indicate net CO<sub>2</sub> uptake by the ecosystem (i.e., CO<sub>2</sub> sink). For



564 consistency, GPP is presented as negative values and Reco as positive. The boxes correspond to  
 565 the 25th and 75th percentiles. The lines denote the 1.5 IQR of the lower and higher quartile,  
 566 where IQR is the inter-quartile range, or distance between the first and third quartiles. There is  
 567 not much chamber data from the boreal regions as they capture NEE only at treeless wetlands.

568

569 **Table 4.** Mean and standard deviation of monthly observations of net ecosystem exchange  
 570 (NEE), gross primary productivity (GPP), and ecosystem respiration (Reco) in  $\text{g C m}^{-2} \text{ month}^{-1}$ .  
 571 Seasons were defined based on the climatological definition (autumn: September-November;  
 572 winter: December-February; spring: March-May; summer: June-August). Positive numbers for  
 573 NEE indicate net  $\text{CO}_2$  loss to the atmosphere (i.e.,  $\text{CO}_2$  source) and negative numbers indicate  
 574 net  $\text{CO}_2$  uptake by the ecosystem (i.e.,  $\text{CO}_2$  sink). For consistency, GPP is presented as negative  
 575 values and Reco as positive.

576

577

578

Biome	Climatological season	Mean monthly NEE	Mean monthly GPP	Mean monthly Reco	Standard deviation of monthly NEE	Standard deviation of monthly GPP	Standard deviation of monthly Reco
Boreal	spring	-5	-40	34	25	49	32
Boreal	summer	-35	-163	124	36	79	71
Boreal	autumn	14	-38	52	18	45	46
Boreal	winter	11	-3	14	8	19	20
Tundra	spring	6	-11	18	9	16	14
Tundra	summer	-26	-72	48	38	60	30



Tundra	autumn	10	-14	21	21	30	15
Tundra	winter	9	-2	12	10	9	11

579

580

#### 581 4. Strengths, limitations, and opportunities

582 ABCflux provides several opportunities for an improved understanding of the ABZ carbon cycle.  
583 It can be used to calculate both short- and longer-term monthly, seasonal, or annual flux  
584 summaries for different regions, or it can be combined with remote sensing and other gridded  
585 data sets to build monthly statistical and process-based models for CO<sub>2</sub> flux upscaling. ABCflux  
586 can further be utilized to study the inter- and intra-annual CO<sub>2</sub> flux variability resulting from  
587 climate and environmental change. The site distribution in ABCflux can also be used to evaluate  
588 the extent of the current flux network and identify under-sampled regions. From a  
589 methodological perspective, data users can compare fluxes estimated with the different  
590 measurement techniques which can help understand the uncertainties associated with individual  
591 techniques. However, there are also some uncertainties that the data user should be aware of  
592 when using ABCflux, which we describe below.

593

##### 594 4.1. Comparing fluxes estimated with different techniques

595 The ABCflux database comprises aggregated observations using eddy covariance, chamber, and  
596 diffusion methods. These methods measure CO<sub>2</sub> fluxes at different spatiotemporal resolutions  
597 and are based on different assumptions. The eddy covariance technique is currently the primary  
598 method to monitor long-term trends in ecosystem CO<sub>2</sub> fluxes (Baldocchi et al., 2018; Baldocchi,  
599 2008), and the majority of observations in ABCflux (79 %) have been made using the technique.  
600 Transforming high-frequency eddy covariance measurements to budgets includes several  
601 processing steps that can, without harmonization and standardization of these steps (Baldocchi et  
602 al., 2001; Pastorello et al., 2020), lead to highly different budget estimates (Soloway et al.,  
603 2017). It is also important to acknowledge that the extent and size of the tower footprint differs  
604 across the sites due to differences in the height of the tower and the direction and magnitude of



605 the wind (Chu et al., 2021). When fluxes are aggregated over longer time periods to cumulative  
606 budgets, one generally assumes the tower footprint remains relatively constant, capturing fluxes  
607 from a similar part of the ecosystem (i.e., the assumption that monthly observations within one  
608 site in ABCflux can be reliably compared with each other); but note that at shorter time periods  
609 this might not be the case (Pirk et al., 2017; Chu et al., 2021).

610

611 The different gas analyzer technologies also play an important role for the fluxes estimated with  
612 the eddy covariance technique. Sites located in the most northern and remote parts of the ABZ  
613 experience a drop in irradiation during autumn and winter which limits solar power availability  
614 for eddy covariance measurements. Closed-path systems require more power to run than open-  
615 path sensors, but open-path sensors are known to have larger uncertainties. For example, open-  
616 path eddy covariance sensors have been shown to incorrectly estimate NEE due to the self-  
617 heating effect of the analyzer, which can result in systematically higher net CO<sub>2</sub> uptake  
618 compared to closed-path sensors (Kittler et al., 2017a); however, this pattern was not clearly  
619 observed in ABCflux when across-site comparisons were made. Furthermore, wintertime fluxes  
620 indicating CO<sub>2</sub> uptake can be erroneous due to the limited ability of the gas analyzer to resolve  
621 very high frequency turbulent eddies (Jentzsch et al., 2021). Recently, some types of open-path  
622 infrared gas analysers have been found to be prone to biases in NEE that scale with sensible heat  
623 fluxes in all seasons rather than with self-heating (Wang et al., 2017; Helbig et al., 2016).

624

625 While using eddy covariance to estimate small-scale spatial variability in NEE is challenging  
626 (McGuire et al., 2012), this can be accomplished with chamber and diffusion techniques.  
627 Chamber measurements can be done in highly heterogeneous environments as long as chamber  
628 closure can be guaranteed; however, most of the chamber measurements in ABCflux have been  
629 conducted in relatively flat and homogeneous graminoid- and wetland-dominated vegetation  
630 types. Most chamber sites in ABCflux include ca.10-20 individual plots in total from ca. 3-5 land  
631 cover types where fluxes are being measured (Virkkala et al., 2018). Chambers can also provide  
632 more direct estimates of Reco and GPP relative to eddy covariance-derived fluxes, and are  
633 therefore useful for estimating the magnitude and range of those component fluxes. However,  
634 manual chamber and diffusion measurements are laborious and have limited temporal  
635 representation, particularly during the non-growing season when they often have only one



636 monthly temporal replicate in ABCflux (McGuire et al., 2012; Fox et al., 2008). Automated  
637 chamber measurements during the non-growing season are also rare in ABCflux.  
638  
639 Because of these methodological differences across the eddy covariance, chamber and diffusion  
640 techniques, comparing fluxes between the methods may result in inconsistencies (Fig. 6). It has  
641 been shown that chamber measurements can be both larger or smaller than the fluxes estimated  
642 with eddy covariance (Phillips et al., 2017). This difference can be related to the uncertainties  
643 with the eddy covariance technique as described above, or to the uncertainties with the chamber  
644 technique (e.g., accurate determination of chamber volume, pressure perturbations, temperature  
645 increase during the measurement, collars disturbing the ground and causing plant root excision).  
646 The differences can also be due to the mismatch between the chamber and tower footprints (<1  
647 m vs. 250–3000 m radii over the measurement equipment, respectively) and the difficulty of  
648 extrapolating local chamber measurements to landscape scales (Marushchak et al., 2013; Fox et  
649 al., 2008). However, several studies have also shown good agreement across the eddy covariance  
650 and chamber measurements (Laine et al., 2006; Wang et al., 2013; Eckhardt et al., 2019; Riutta  
651 et al., 2007). Potential mismatches may also be due to a bias towards daytime measurements in  
652 manual chamber measurements (see field “Diurnal\_coverage”). During daytime, plants are  
653 actively photosynthesizing whereas respiration is the dominant flux at night (López-Blanco et al.,  
654 2017). Presumably because of these day vs. night-time differences, we observed stronger sink  
655 strength in manual chamber measurements compared to other flux measurements in ABCflux,  
656 even though eddy covariance measurements have also been observed to underestimate night-time  
657 CO<sub>2</sub> loss. This underestimation in night-time eddy covariance measurements is due to suppressed  
658 turbulent exchange linked to stable atmospheric stratification, and systematic biases due to  
659 horizontal advection (Aubinet et al., 2012). Despite these uncertainties, including fluxes  
660 estimated with all of these techniques into one database improves the understanding of  
661 underlying variability of landscape-scale flux estimates. Indeed, there are roughly 10 sites in  
662 ABCflux that include both eddy covariance and chamber/diffusion measurements conducted at  
663 the same time. These observations might not have identical site coordinates but they are often  
664 very close to each other (<500 m away from each other). Including multiple methods from the  
665 same site provides an opportunity to compare estimates from different methods over a larger  
666 number of sites.



667

668 4.2. Uncertainties in eddy covariance flux partitioning

669 Monthly Reco and GPP fluxes derived from eddy covariance were primarily estimated using flux  
670 partitioning based on night-time Reco based on the assumption that during night, NEE measured  
671 at low PAR is equivalent to Reco (Reichstein et al., 2005). Focusing on night-time partitioning  
672 ensured that data from older sites using this partitioning method could be included, and that most  
673 of the fluxes were standardized using one common partitioning method. However, particularly at  
674 sites at higher latitudes of the ABZ, low-light night-time conditions are restricted to rather short  
675 periods during summer, limiting the database for assessing Reco rates and therefore increasing  
676 uncertainties associated with the night-time partitioning (López-Blanco et al., 2020). Recent  
677 research suggests that other methods such as daytime partitioning (Lasslop et al. 2010), and even  
678 more recently artificial neural networks (ANN) (Tramontana et al., 2020), might be more  
679 accurate methods for flux partitioning by addressing the assumptions from night-time  
680 partitioning methods (Pastorello et al., 2020; Papale et al., 2006; Reichstein et al., 2005; Keenan  
681 et al., 2019). Specifically, the assumption of a constant diel temperature sensitivity during night-  
682 and daytime might introduce error in eddy covariance-based Reco estimates extrapolated from  
683 night-time measurements (Järveoja et al., 2020; Keenan et al., 2019). It should be noted that  
684 ABCflux database used night-time partitioning of fluxes extracted from repositories for  
685 consistency; however, fluxes contributed by some databases, PIs or extracted from papers may  
686 be based on other partitioning methods, as noted in the database. In a few cases, observations  
687 from the same site were based on different partitioning methods, which limits the usage of data  
688 at those sites for time-series exploration. These different gap-filling and partitioning approaches  
689 can impact the magnitude of monthly CO<sub>2</sub> budgets. For example, a study comparing four gap-  
690 filling methods in a boreal forest showed that the 14-year average annual NEE budget varied  
691 from 4 to 48 g C m<sup>-2</sup> year<sup>-1</sup> depending on the gap-filling approach (Soloway et al., 2017).  
692 However, a comparison of multiple gap-filling and partitioning methods across sites showed that  
693 variation in annual GPP and Reco between partitioning methods was small (Desai et al., 2008),  
694 which provides confidence in estimates from partitioned GPP and Reco components from the  
695 differing methods used in this database.

696





697

698 We suggest data users remain cautious when using ABCflux data to understand mechanistic  
699 relationships between meteorological variables and fluxes, as the gap-filled and partitioned  
700 monthly fluxes already include some information about, for example, air or soil temperatures and  
701 light conditions. To completely avoid circularity in these exploratory analyses, we recommend  
702 data users download the original and non-gap filled NEE records, or download fluxes partitioned  
703 in a way that is consistent and biologically relevant for the particular research question from flux  
704 repositories.

705

#### 706 4.3. Representativeness and completeness of the data

707 The ABCflux database site distribution covers all vegetation types and countries within the ABZ.  
708 However, there are regional and temporal biases in the database due to the differences in  
709 accessibility for sampling certain regions (also documented in (Virkkala et al., 2019)). As a  
710 result, the number of monthly observations does not always correlate with the size of the  
711 country/region or vegetation type. For example, Russia and Canada cover in total ca. 80 % of the  
712 ABZ but include only ca. 40 % of the monthly observations. While the distribution of these  
713 measurements seems to be rather balanced between the Russian tundra and boreal biomes,  
714 Canadian observations are primarily located in the boreal biome, largely due to the high amount  
715 of measurements conducted as part of the Boreal Ecosystem-Atmosphere Study (Sellers et al.,  
716 1997). Deciduous needleleaf (i.e., larch) forests, the primary vegetation type in central and  
717 eastern Siberia, has the smallest amount of data compared to its area (<5 % of monthly  
718 observations vs. >20 % coverage of the ABZ). Additional data gaps are located in barren and  
719 prostrate-shrub tundra and sparse boreal vegetation. Eddy covariance towers in mountainous  
720 regions are also rare as eddy covariance towers are most often set up over homogeneous and flat  
721 terrains to avoid advection (Baldocchi, 2003; Etzold et al., 2010). Alaska and Finland cover <10  
722 % of the ABZ but include >40 % of the monthly observations. Sites with NEE observations have  
723 the largest geographical coverage, with less availability for partitioned GPP and Reco fluxes.  
724 Therefore, regional summaries of Reco and GPP do not sum up to NEE. Moreover, although the  
725 oldest records in ABCflux originate from 1989, observations from the 1990s are primarily  
726 located in a few boreal or Alaskan tundra sites. The measurement records from tundra sites are



727 shorter than boreal sites over the full time span of the database, and it is therefore more uncertain  
728 to investigate long-term temporal changes in tundra fluxes. Finally, the lowest amount of flux  
729 data in ABCflux is from winter, which is the most challenging period for data collection in high  
730 latitudes (Kittler et al., 2017b; Jentzsch et al., 2021). Fluxes are generally small during this  
731 period (Natali et al., 2019), leading to higher relative uncertainties in flux estimation compared  
732 to other seasons. These regional and temporal biases need to be considered in future analyses to  
733 assure the robustness of our understanding of C fluxes across the ABZ.

734

735 Although ABCflux includes a comprehensive compilation of flux and supporting environmental  
736 and methodological information, the information is not exhaustive. We acknowledge that this  
737 database is missing some eddy covariance sites that were recently summarized in a tower survey  
738 (see preliminary results in <https://cosima.nceas.ucsb.edu/carbon-flux-sites/>), because these data  
739 were unavailable at the time of database compilation. Moreover, the overall quality or the gap-  
740 filled percentage of the eddy covariance observations is not reported for each eddy covariance  
741 site, limiting the potential to explore the effects of data quality on fluxes across all the eddy  
742 covariance sites. Comparing soil temperature or moisture across sites has uncertainties due to  
743 differences in sensor depths, which are not always reported in the database. We hope to improve  
744 and increase the flux and supporting data in the future as new data are being collected, for  
745 example, by leveraging the ONEflux pipeline and its different outputs (Pastorello et al., 2020), as  
746 well as aggregating new measurements that are not part of any networks.

## 747 5. Data use guidelines

748 Data are publicly available using a Creative Commons Attribution 4.0 International copyright  
749 (CC BY 4.0). Data are fully public, but should be appropriately referenced by citing this paper  
750 and the database (see Section 6). We suggest that researchers planning to use this database as a  
751 core dataset for their analysis contact and collaborate with the database developers and relevant  
752 individual site contributors.

## 753 6. Data availability and access

754 The database associated with this publication can be found at Virkkala et al. 2021a  
755 (<https://doi.org/10.3334/ORNLDAAAC/1934>).



## 756 7. Conclusions

757 ABCflux provides the most comprehensive database of ABZ terrestrial ecosystem CO<sub>2</sub> fluxes to  
758 date. It is particularly useful for future modeling, remote sensing, and empirical studies aiming to  
759 understand CO<sub>2</sub> budgets and regional variability in flux magnitudes, as well as changes in fluxes  
760 through time. It can also be used to understand how different environmental conditions influence  
761 fluxes, and to better understand the current extent of the flux measurement network and its  
762 representativeness across the Arctic-Boreal region.

## 763 8. Author contributions

764 The ABCflux database was conceptualized and developed by a team led by SMN, BMR, JDW,  
765 MM, AMV, and EAGS, with additional comments from OS. KS and SJC compiled the data, with  
766 contributions from AMV, MM, DP, CM, and JN, and data screening by AMV and SMN. AMV  
767 drafted and coordinated the manuscript in close collaboration with SMN, BMR, JDW, KS, and  
768 MM. All authors contributed to the realization of the ABCflux database and participated in the  
769 editing of the manuscript. PIs whose data were extracted from publications are not coauthors in  
770 this paper, unless new data were provided, but their contact details can be found in the database.

## 771 9. Competing interests

772 The authors declare that they have no conflict of interest.

## 773 10. Acknowledgements

774 AMV, BMR, SMN, and JDW were funded by the Gordon and Betty Moore Foundation (grant  
775 #8414). BMR, KS, SJC, CM, and JN were also funded by the NASA Carbon Cycle Science and  
776 Arctic-Boreal Vulnerability Experiment programs (ABoVE grant NNX17AE13G), SMN by  
777 NASA ABoVE (grant NNX15AT81A) and JDW by NNX15AT81A and NASA NIP grant  
778 NNH17ZDA001N. EAGS acknowledges NSF Research, Synthesis, and Knowledge Transfer in a  
779 Changing Arctic: Science Support for the Study of Environmental Arctic Change (grant  
780 #1331083) and NSF PLR Arctic System Science Research Networking Activities (Permafrost  
781 Carbon Network: Synthesizing Flux Observations for Benchmarking Model Projections of  
782 Permafrost Carbon Exchange; grant #1931333. EAGS further acknowledges US Department of



783 Energy and Denali National Park. MBN and MP acknowledge Swedish ICOS (Integrated Carbon  
784 Observatory System) funded by VR and contributing institutions; SITES (Swedish Infrastructure  
785 for Ecosystem Science) funded by VR and contributing institutions; VR (grant # 2018-03966 and  
786 # 2019-04676), FORMAS (grant # 2016-01289), and Kempe Foundations (SMK-1211). EE, CE,  
787 and MSB-H was funded by NSF Arctic Observatory Network and CAG, VSL, EH by Natural  
788 Sciences and Engineering Research Council. IM, PK, EST, AL acknowledges ICOS-Finland and  
789 AV Russian Science Foundation, project 21-14-00209. AL, MA, TL, J-PT, and JH further  
790 acknowledge Ministry of transport and communication. WQ, EE, VSL were funded by  
791 ArcticNet. HK acknowledges The Arctic Challenge for Sustainability and The Arctic Challenge  
792 for Sustainability II (JPMXD1420318865), MEM the Academy of Finland project PANDA  
793 (decision no. 317054) and CV the Academy of Finland project MUFFIN (decision no. 332196).  
794 NN acknowledges Arctic Data Center, National Science Foundation, US Department of Energy,  
795 Denali National Park. YM was funded by Ministry of Environment, Japan and MU by the Arctic  
796 Challenge for Sustainability II (ArCS II; JPMXD1420318865) and KAKENHI (19H05668).  
797 SFO acknowledges US National Science Foundation, and MiM, BE, TRC Greenland Ecosystem  
798 Monitoring program. BE further acknowledge Arctic Station, University of Copenhagen and the  
799 Danish National Research Foundation (CENPERM DNRF100). ELB was funded by "Greenland  
800 Research Council, grant number 80.35, financed by the "Danish Program for Arctic Research",  
801 and LM by TCOS Siberia. DH and LK were funded by Deutsche Forschungsgemeinschaft under  
802 Germany's Excellence Strategy – EXC 177 'CliSAP - Integrated Climate System Analysis and  
803 Prediction'. JJ acknowledges Swedish Forest Society Foundation (2018-485-Steig 2 2017) and  
804 FORMAS (2018-00792). DZ was funded by National Science Foundation (NSF) (award number  
805 1204263, and 1702797) NASA ABoVE (NNX15AT74A; NNX16AF94A) Program, Natural  
806 Environment Research Council (NERC) UAMS Grant (NE/P002552/1), NOAA Cooperative  
807 Science Center for Earth System Sciences and Remote Sensing Technologies (NOAA-  
808 CESSRST) under the Cooperative Agreement Grant # NA16SEC4810008, European Union's  
809 Horizon 2020 research and innovation program under grant agreement No. 72789. S-JP was  
810 funded by National Research Foundation of Korea Grant from the Korean Government (NRF-  
811 2021M1A5A1065425, KOPRI-PN21011). NC acknowledges "National Research Foundation of  
812 Korea Grant from the Korean Government (MSIT; the Ministry of Science and ICT) (NRF-  
813 2021M1A5A1065679 and NRF-2021R111A1A01053870)". SD was funded by Department of



814 Energy and NGEE- Arctic. FJWP is funded by the Swedish Research Council (registration nr.  
815 2017-05268) and the Research Council of Norway (grant no. 274711). The authors would like to  
816 acknowledge Tiffany Windholz for her work on standardizing and cleaning up the database.

## 817 References

- 818 Natural Earth - Free vector and raster map data at 1:10m, 1:50m, and 1:110m scales:  
819 <https://www.naturalearthdata.com/>, last access: 12 February 2021.
- 820 Reconciling historical and contemporary trends in terrestrial carbon exchange of the northern  
821 permafrost-zone: [https://arcticdata.io/reconciling-historical-and-contemporary-trends-in-](https://arcticdata.io/reconciling-historical-and-contemporary-trends-in-terrestrial-carbon-exchange-of-the-northern-permafrost-zone/)  
822 [terrestrial-carbon-exchange-of-the-northern-permafrost-zone/](https://arcticdata.io/reconciling-historical-and-contemporary-trends-in-terrestrial-carbon-exchange-of-the-northern-permafrost-zone/), last access: 11 February 2021.
- 823 Aubinet, M., Vesala, T., and Papale, D.: Eddy Covariance: A Practical Guide to Measurement  
824 and Data Analysis, Springer Science & Business Media, 438 pp., 2012.
- 825 Baldocchi, D.: “Breathing” of the terrestrial biosphere: lessons learned from a global network of  
826 carbon dioxide flux measurement systems, *Aust. J. Bot.*, 56, 1–26, 2008.
- 827 Baldocchi, D., Falge, E., Gu, L., Olson, R., Hollinger, D., Running, S., Anthoni, P., Bernhofer,  
828 C., Davis, K., Evans, R., Fuentes, J., Goldstein, A., Katul, G., Law, B., Lee, X., Malhi, Y.,  
829 Meyers, T., Munger, W., Oechel, W., Paw U, K. T., Pilegaard, K., Schmid, H. P., Valentini, R.,  
830 Verma, S., Vesala, T., Wilson, K., and Wofsy, S.: FLUXNET: A New Tool to Study the  
831 Temporal and Spatial Variability of Ecosystem-Scale Carbon Dioxide, Water Vapor, and Energy  
832 Flux Densities, *Bull. Am. Meteorol. Soc.*, 82, 2415–2434, [https://doi.org/10.1175/1520-](https://doi.org/10.1175/1520-0477(2001)082<2415:FANTTS>2.3.CO;2)  
833 [0477\(2001\)082<2415:FANTTS>2.3.CO;2](https://doi.org/10.1175/1520-0477(2001)082<2415:FANTTS>2.3.CO;2), 2001.
- 834 Baldocchi, D., Chu, H., and Reichstein, M.: Inter-annual variability of net and gross ecosystem  
835 carbon fluxes: A review, *Agric. For. Meteorol.*, 249, 520–533,  
836 <https://doi.org/10.1016/j.agrformet.2017.05.015>, 2018.
- 837 Baldocchi, D. D.: Assessing the eddy covariance technique for evaluating carbon dioxide  
838 exchange rates of ecosystems: past, present and future, [https://doi.org/10.1046/j.1365-](https://doi.org/10.1046/j.1365-2486.2003.00629.x)  
839 [2486.2003.00629.x](https://doi.org/10.1046/j.1365-2486.2003.00629.x), 2003.
- 840 Belshe, E. F., Schuur, E. A. G., and Bolker, B. M.: Tundra ecosystems observed to be CO<sub>2</sub>  
841 sources due to differential amplification of the carbon cycle, *Ecol. Lett.*, 16, 1307–1315,  
842 <https://doi.org/10.1111/ele.12164>, 2013.
- 843 Björkman, M. P., Morgner, E., Björk, R. G., Cooper, E. J., Elberling, B., and Klemetsson, L.: A  
844 comparison of annual and seasonal carbon dioxide effluxes between sub-Arctic Sweden and  
845 High-Arctic Svalbard, *Polar Res.*, 29, 75–84, <https://doi.org/10.1111/j.1751-8369.2010.00150.x>,  
846 2010a.
- 847 Björkman, M. P., Morgner, E., Cooper, E. J., Elberling, B., Klemetsson, L., and Björk, R. G.:



- 848 Winter carbon dioxide effluxes from Arctic ecosystems: An overview and comparison of  
849 methodologies: WINTER CO<sub>2</sub>EFFLUXES FROM ARCTIC SOILS, *Global Biogeochem.*  
850 *Cycles*, 24, <https://doi.org/10.1029/2009gb003667>, 2010b.
- 851 Bond-Lamberty, B., Christianson, D. S., Malhotra, A., Pennington, S. C., Sihi, D.,  
852 AghaKouchak, A., Anjileli, H., Altaf Arain, M., Armesto, J. J., Ashraf, S., Ataka, M., Baldocchi,  
853 D., Andrew Black, T., Buchmann, N., Carbone, M. S., Chang, S.-C., Crill, P., Curtis, P. S.,  
854 Davidson, E. A., Desai, A. R., Drake, J. E., El-Madany, T. S., Gavazzi, M., Görres, C.-M.,  
855 Gough, C. M., Goulden, M., Gregg, J., Gutiérrez Del Arroyo, O., He, J.-S., Hirano, T., Hoppo,  
856 A., Hughes, H., Järveoja, J., Jassal, R., Jian, J., Kan, H., Kaye, J., Kominami, Y., Liang, N.,  
857 Lipson, D., Macdonald, C. A., Maseyk, K., Mathes, K., Mauritz, M., Mayes, M. A., McNulty, S.,  
858 Miao, G., Migliavacca, M., Miller, S., Miniati, C. F., Nietz, J. G., Nilsson, M. B., Noormets, A.,  
859 Norouzi, H., O’Connell, C. S., Osborne, B., Oyonarte, C., Pang, Z., Peichl, M., Pendall, E.,  
860 Perez-Quezada, J. F., Phillips, C. L., Phillips, R. P., Raich, J. W., Renchon, A. A., Ruehr, N. K.,  
861 Sánchez-Cañete, E. P., Saunders, M., Savage, K. E., Schrumppf, M., Scott, R. L., Seibt, U., Silver,  
862 W. L., Sun, W., Szutu, D., Takagi, K., Takagi, M., Teramoto, M., Tjoelker, M. G., Trumbore, S.,  
863 Ueyama, M., Vargas, R., Varner, R. K., Verfaillie, J., Vogel, C., Wang, J., Winston, G., Wood,  
864 T. E., Wu, J., Wutzler, T., Zeng, J., Zha, T., Zhang, Q., and Zou, J.: COSORE: A community  
865 database for continuous soil respiration and other soil-atmosphere greenhouse gas flux data,  
866 *Glob. Chang. Biol.*, 26, 7268–7283, <https://doi.org/10.1111/gcb.15353>, 2020.
- 867 Box, J. E., Colgan, W. T., Christensen, T. R., Schmidt, N. M., Lund, M., Parmentier, F.-J. W.,  
868 Brown, R., Bhatt, U. S., Euskirchen, E. S., Romanovsky, V. E., Walsh, J. E., Overland, J. E.,  
869 Wang, M., Corell, R. W., Meier, W. N., Wouters, B., Mernild, S., Mård, J., Pawlak, J., and  
870 Olsen, M. S.: Key indicators of Arctic climate change: 1971–2017, *Environ. Res. Lett.*, 14,  
871 045010, <https://doi.org/10.1088/1748-9326/aafc1b>, 2019.
- 872 Cahoon, S. M. P., Sullivan, P. F., and Post, E.: Greater Abundance of *Betula nana* and Early  
873 Onset of the Growing Season Increase Ecosystem CO<sub>2</sub> Uptake in West Greenland, *Ecosystems*,  
874 19, 1149–1163, <https://doi.org/10.1007/s10021-016-9997-7>, 2016.
- 875 Chu, H., Luo, X., Ouyang, Z., Chan, W. S., Dengel, S., Biraud, S. C., Torn, M. S., Metzger, S.,  
876 Kumar, J., Arain, M. A., Arkebauer, T. J., Baldocchi, D., Bernacchi, C., Billesbach, D., Black, T.  
877 A., Blanken, P. D., Bohrer, G., Bracho, R., Brown, S., Brunsell, N. A., Chen, J., Chen, X., Clark,  
878 K., Desai, A. R., Duman, T., Durden, D., Fares, S., Forbrich, I., Gamon, J. A., Gough, C. M.,  
879 Griffis, T., Helbig, M., Hollinger, D., Humphreys, E., Ikawa, H., Iwata, H., Ju, Y., Knowles, J.  
880 F., Knox, S. H., Kobayashi, H., Kolb, T., Law, B., Lee, X., Litvak, M., Liu, H., Munger, J. W.,  
881 Noormets, A., Novick, K., Oberbauer, S. F., Oechel, W., Oikawa, P., Papuga, S. A., Pendall, E.,  
882 Prajapati, P., Prueger, J., Quinton, W. L., Richardson, A. D., Russell, E. S., Scott, R. L., Starr,  
883 G., Staebler, R., Stoy, P. C., Stuart-Haëntjens, E., Sonntag, O., Sullivan, R. C., Suyker, A.,  
884 Ueyama, M., Vargas, R., Wood, J. D., and Zona, D.: Representativeness of Eddy-Covariance  
885 flux footprints for areas surrounding AmeriFlux sites, *Agric. For. Meteorol.*, 301-302, 108350,  
886 <https://doi.org/10.1016/j.agrformet.2021.108350>, 2021.
- 887 Desai, A. R., Richardson, A. D., Moffat, A. M., Kattge, J., Hollinger, D. Y., Barr, A., Falge, E.,  
888 Noormets, A., Papale, D., Reichstein, M., and Stauch, V. J.: Cross-site evaluation of eddy  
889 covariance GPP and RE decomposition techniques, *Agric. For. Meteorol.*, 148, 821–838,



- 890 <https://doi.org/10.1016/j.agrformet.2007.11.012>, 2008.
- 891 Dinerstein, E., Olson, D., Joshi, A., Vynne, C., Burgess, N. D., Wikramanayake, E., Hahn, N.,  
892 Palminteri, S., Hedao, P., Noss, R., Hansen, M., Locke, H., Ellis, E. C., Jones, B., Barber, C. V.,  
893 Hayes, R., Kormos, C., Martin, V., Crist, E., Sechrest, W., Price, L., Baillie, J. E. M., Weeden,  
894 D., Suckling, K., Davis, C., Sizer, N., Moore, R., Thau, D., Birch, T., Potapov, P., Turubanova,  
895 S., Tyukavina, A., de Souza, N., Pintea, L., Brito, J. C., Llewellyn, O. A., Miller, A. G., Patzelt,  
896 A., Ghazanfar, S. A., Timberlake, J., Klöser, H., Shennan-Farpón, Y., Kindt, R., Lillesø, J.-P. B.,  
897 van Breugel, P., Graudal, L., Voge, M., Al-Shammari, K. F., and Saleem, M.: An Ecoregion-  
898 Based Approach to Protecting Half the Terrestrial Realm, *Bioscience*, 67, 534–545,  
899 <https://doi.org/10.1093/biosci/bix014>, 2017.
- 900 Eckhardt, T., Knoblauch, C., Kutzbach, L., Holl, D., Simpson, G., Abakumov, E., and Pfeiffer,  
901 E.-M.: Partitioning net ecosystem exchange of CO<sub>2</sub> on the pedon scale in the Lena River Delta,  
902 Siberia, *Biogeosciences*, 16, 1543–1562, <https://doi.org/10.5194/bg-16-1543-2019>, 2019.
- 903 Etzold, S., Buchmann, N., and Eugster, W.: Contribution of advection to the carbon budget  
904 measured by eddy covariance at a steep mountain slope forest in Switzerland, *Biogeosciences*, 7,  
905 2461–2475, <https://doi.org/10.5194/bg-7-2461-2010>, 2010.
- 906 Euskirchen, E. S., Bret-Harte, M. S., Scott, G. J., Edgar, C., and Shaver, G. R.: Seasonal patterns  
907 of carbon dioxide and water fluxes in three representative tundra ecosystems in northern Alaska,  
908 *Ecosphere*, 3, art4, <https://doi.org/10.1890/es11-00202.1>, 2012.
- 909 Fox, A. M., Huntley, B., Lloyd, C. R., Williams, M., and Baxter, R.: Net ecosystem exchange  
910 over heterogeneous Arctic tundra: Scaling between chamber and eddy covariance measurements,  
911 *Global Biogeochem. Cycles*, 22, 2008.
- 912 Gorham, E.: Northern Peatlands: Role in the Carbon Cycle and Probable Responses to Climatic  
913 Warming, *Ecol. Appl.*, 1, 182–195, <https://doi.org/10.2307/1941811>, 1991.
- 914 Hari, P., Nikinmaa, E., Pohja, T., Siivola, E., Bäck, J., Vesala, T., and Kulmala, M.: Station for  
915 Measuring Ecosystem-Atmosphere Relations: SMEAR, in: *Physical and Physiological Forest  
916 Ecology*, edited by: Hari, P., Heliövaara, K., and Kulmala, L., Springer Netherlands, Dordrecht,  
917 471–487, [https://doi.org/10.1007/978-94-007-5603-8\\_9](https://doi.org/10.1007/978-94-007-5603-8_9), 2013.
- 918 Helbig, M., Wischniewski, K., Gosselin, G. H., Biraud, S. C., Bogoev, I., Chan, W. S.,  
919 Euskirchen, E. S., Glenn, A. J., Marsh, P. M., Quinton, W. L., and Sonntag, O.: Addressing a  
920 systematic bias in carbon dioxide flux measurements with the EC150 and the IRGASON open-  
921 path gas analyzers, *Agric. For. Meteorol.*, 228–229, 349–359,  
922 <https://doi.org/10.1016/j.agrformet.2016.07.018>, 2016.
- 923 Hermle, S., Lavigne, M. B., Bernier, P. Y., Bergeron, O., and Paré, D.: Component respiration,  
924 ecosystem respiration and net primary production of a mature black spruce forest in northern  
925 Quebec, *Tree Physiol.*, 30, 527–540, <https://doi.org/10.1093/treephys/tpq002>, 2010.
- 926 Hugelius, G., Strauss, J., Zubrzycki, S., Harden, J. W., Schuur, E. A. G., Ping, C.-L.,  
927 Schirmer, L., Grosse, G., Michaelson, G. J., Koven, C. D., and Others: Estimated stocks of



- 928 circumpolar permafrost carbon with quantified uncertainty ranges and identified data gaps,  
929 *Biogeosciences*, 11, 2014.
- 930 Hugelius, G., Loisel, J., Chadburn, S., Jackson, R. B., Jones, M., MacDonald, G., Marushchak,  
931 M., Olefeldt, D., Packalen, M., Siewert, M. B., Treat, C., Turetsky, M., Voigt, C., and Yu, Z.:  
932 Large stocks of peatland carbon and nitrogen are vulnerable to permafrost thaw, *Proc. Natl.*  
933 *Acad. Sci. U. S. A.*, 117, 20438–20446, <https://doi.org/10.1073/pnas.1916387117>, 2020.
- 934 Järveoja, J., Nilsson, M. B., Gažovič, M., Crill, P. M., and Peichl, M.: Partitioning of the net CO  
935 2 exchange using an automated chamber system reveals plant phenology as key control of  
936 production and respiration fluxes in a boreal peatland, *Glob. Chang. Biol.*, 24, 3436–3451, 2018.
- 937 Järveoja, J., Nilsson, M. B., Crill, P. M., and Peichl, M.: Bimodal diel pattern in peatland  
938 ecosystem respiration rebuts uniform temperature response, *Nat. Commun.*, 11, 4255,  
939 <https://doi.org/10.1038/s41467-020-18027-1>, 2020.
- 940 Jentsch, K., Schulz, A., Pirk, N., Foken, T., Crewell, S., and Boike, J.: High levels of CO 2  
941 exchange during synoptic-scale events introduce large uncertainty into the arctic carbon budget,  
942 *Geophys. Res. Lett.*, 48, <https://doi.org/10.1029/2020gl092256>, 2021.
- 943 Jian, J., Vargas, R., Anderson-Teixeira, K., Stell, E., Herrmann, V., Horn, M., Kholod, N.,  
944 Manzoni, J., Marchesi, R., Paredes, D., and Others: A restructured and updated global soil  
945 respiration database (SRDB-V5), 1–19, 2020.
- 946 Keenan, T. F. and Williams, C. A.: The Terrestrial Carbon Sink, *Annu. Rev. Environ. Resour.*,  
947 43, 219–243, <https://doi.org/10.1146/annurev-environ-102017-030204>, 2018.
- 948 Keenan, T. F., Migliavacca, M., Papale, D., Baldocchi, D., Reichstein, M., Torn, M., and  
949 Wutzler, T.: Widespread inhibition of daytime ecosystem respiration, *Nat Ecol Evol*, 3, 407–415,  
950 <https://doi.org/10.1038/s41559-019-0809-2>, 2019.
- 951 Kittler, F., Eugster, W., Foken, T., Heimann, M., Kolle, O., and Göckede, M.: High-quality  
952 eddy-covariance CO2 budgets under cold climate conditions: Arctic Eddy-Covariance  
953 CO2 Budgets, *J. Geophys. Res. Biogeosci.*, 122, 2064–2084,  
954 <https://doi.org/10.1002/2017jg003830>, 2017a.
- 955 Kittler, F., Heimann, M., Kolle, O., Zimov, N., Zimov, S., and Göckede, M.: Long-term drainage  
956 reduces CO2 uptake and CH4 emissions in a Siberian permafrost ecosystem, *Global*  
957 *Biogeochem. Cycles*, 31, 1704–1717, 2017b.
- 958 Laine, A., Sottocornola, M., Kiely, G., Byrne, K. A., Wilson, D., and Tuittila, E.-S.: Estimating  
959 net ecosystem exchange in a patterned ecosystem: Example from blanket bog, *Agric. For.*  
960 *Meteorol.*, 138, 231–243, <https://doi.org/10.1016/j.agrformet.2006.05.005>, 2006.
- 961 Lamarche, C., Bontemps, S., Verhegghen, A., Radoux, J., Vanbogaert, E., Kalogirou, V., Seifert,  
962 F. M., Arino, O., and Defourny, P.: Characterizing The Surface Dynamics For Land Cover  
963 Mapping: Current Achievements Of The ESA CCI Land Cover, 72279, 2013.





- 964 Lasslop, G., Reichstein, M., Papale, D., Richardson, A. D., Arneeth, A., Barr, A., Stoy, P., and  
965 Wohlfahrt, G.: Separation of net ecosystem exchange into assimilation and respiration using a  
966 light response curve approach: critical issues and global evaluation: SEPARATION OF NEE  
967 INTO GPP AND RECO, *Glob. Chang. Biol.*, 16, 187–208, <https://doi.org/10.1111/j.1365-2486.2009.02041.x>, 2010.
- 969 López-Blanco, E., Lund, M., Williams, M., Tamstorf, M. P., Westergaard-Nielsen, A., Exbrayat,  
970 J.-F., Hansen, B. U., and Christensen, T. R.: Exchange of CO<sub>2</sub> in Arctic tundra: impacts of  
971 meteorological variations and biological disturbance, *Biogeosciences*, 14, 4467–4483,  
972 <https://doi.org/10.5194/bg-14-4467-2017>, 2017.
- 973 López-Blanco, E., Jackowicz-Korczynski, M., Mastepanov, M., Skov, K., Westergaard-Nielsen,  
974 A., Williams, M., and Christensen, T. R.: Multi-year data-model evaluation reveals the  
975 importance of nutrient availability over climate in arctic ecosystem C dynamics, *Environ. Res. Lett.*, 15, 094007, <https://doi.org/10.1088/1748-9326/ab865b>, 2020.
- 977 Luysaert, S., Inglima, I., Jung, M., Richardson, A. D., Reichstein, M., Papale, D., Piao, S. L.,  
978 Schulze, E.-D., Wingate, L., Matteucci, G., Aragao, L., Aubinet, M., Beer, C., Bernhofer, C.,  
979 Black, K. G., Bonal, D., Bonnefond, J.-M., Chambers, J., Ciais, P., Cook, B., Davis, K. J.,  
980 Dolman, A. J., Gielen, B., Goulden, M., Grace, J., Granier, A., Grelle, A., Griffis, T., Grünwald,  
981 T., Guidolotti, G., Hanson, P. J., Harding, R., Hollinger, D. Y., Hutryra, L. R., Kolari, P., Kruijt,  
982 B., Kutsch, W., Lagergren, F., Laurila, T., Law, B. E., Le Maire, G., Lindroth, A., Loustau, D.,  
983 Malhi, Y., Mateus, J., Migliavacca, M., Misson, L., Montagnani, L., Moncrieff, J., Moors, E.,  
984 Munger, J. W., Nikinmaa, E., Ollinger, S. V., Pita, G., Rebmann, C., Roupsard, O., Saigusa, N.,  
985 Sanz, M. J., Seufert, G., Sierra, C., Smith, M.-L., Tang, J., Valentini, R., Vesala, T., and  
986 Janssens, I. A.: CO<sub>2</sub> balance of boreal, temperate, and tropical forests derived from a global  
987 database, *Glob. Chang. Biol.*, 13, 2509–2537, <https://doi.org/10.1111/j.1365-2486.2007.01439.x>,  
988 2007.
- 989 Marushchak, M. E., Kiepe, I., Biasi, C., Elsakov, V., Friborg, T., Johansson, T., Soegaard, H.,  
990 Virtanen, T., and Martikainen, P. J.: Carbon dioxide balance of subarctic tundra from plot to  
991 regional scales, <https://doi.org/10.5194/bg-10-437-2013>, 2013.
- 992 McGuire, A. D., Christensen, T. R., Hayes, D. J., Heroult, A., Euskirchen, E., Yi, Y., Kimball, J.  
993 S., Koven, C., Lafleur, P., Miller, P. A., Oechel, W., Peylin, P., and Williams, M.: An assessment  
994 of the carbon balance of arctic tundra: comparisons among observations, process models, and  
995 atmospheric inversions, *Biogeosci. Discuss.*, 9, 4543, <https://doi.org/10.5194/bg-9-3185-2012>,  
996 2012.
- 997 McGuire, A. D., Koven, C., Lawrence, D. M., Clein, J. S., Xia, J., Beer, C., Burke, E., Chen, G.,  
998 Chen, X., Delire, C., Jafarov, E., MacDougall, A. H., Marchenko, S., Nicolsky, D., Peng, S.,  
999 Rinke, A., Saito, K., Zhang, W., Alkama, R., Bohn, T. J., Ciais, P., Decharme, B., Ekici, A.,  
1000 Gouttevin, I., Hajima, T., Hayes, D. J., Ji, D., Krinner, G., Lettenmaier, D. P., Luo, Y., Miller, P.  
1001 A., Moore, J. C., Romanovsky, V., Schädel, C., Schaefer, K., Schuur, E. A. G., Smith, B.,  
1002 Sueyoshi, T., and Zhuang, Q.: Variability in the sensitivity among model simulations of  
1003 permafrost and carbon dynamics in the permafrost region between 1960 and 2009, *Global  
1004 Biogeochem. Cycles*, 30, 1015–1037, <https://doi.org/10.1002/2016GB005405>, 2016.



- 1005 Merbold, L., Kutsch, W. L., Corradi, C., Kolle, O., Rebmann, C., Stoy, P. C., Zimov, S. A., and  
1006 Schulze, E.-D.: Artificial drainage and associated carbon fluxes (CO<sub>2</sub>/CH<sub>4</sub>) in a tundra  
1007 ecosystem, *Glob. Chang. Biol.*, 15, 2599–2614, <https://doi.org/10.1111/j.1365->  
1008 2486.2009.01962.x, 2009.
- 1009 Mishra, U., Hugelius, G., Shelef, E., Yang, Y., Strauss, J., Lupachev, A., Harden, J. W., Jastrow,  
1010 J. D., Ping, C.-L., Riley, W. J., Schuur, E. A. G., Matamala, R., Siewert, M., Nave, L. E., Koven,  
1011 C. D., Fuchs, M., Palmtag, J., Kuhry, P., Treat, C. C., Zubrzycki, S., Hoffman, F. M., Elberling,  
1012 B., Camill, P., Veremeeva, A., and Orr, A.: Spatial heterogeneity and environmental predictors  
1013 of permafrost region soil organic carbon stocks, *Sci Adv*, 7,  
1014 <https://doi.org/10.1126/sciadv.aaz5236>, 2021.
- 1015 Natali, S. M., Watts, J. D., Rogers, B. M., Potter, S., Ludwig, S. M., Selbmann, A.-K., Sullivan,  
1016 P. F., Abbott, B. W., Arndt, K. A., Birch, L., Björkman, M. P., Bloom, A. A., Celis, G.,  
1017 Christensen, T. R., Christiansen, C. T., Commane, R., Cooper, E. J., Crill, P., Czimczik, C.,  
1018 Davydov, S., Du, J., Egan, J. E., Elberling, B., Euskirchen, E. S., Friborg, T., Genet, H.,  
1019 Göckede, M., Goodrich, J. P., Grogan, P., Helbig, M., Jafarov, E. E., Jastrow, J. D., Kalthori, A.  
1020 A. M., Kim, Y., Kimball, J. S., Kutzbach, L., Lara, M. J., Larsen, K. S., Lee, B.-Y., Liu, Z.,  
1021 Lorant, M. M., Lund, M., Lupascu, M., Madani, N., Malhotra, A., Matamala, R., McFarland, J.,  
1022 McGuire, A. D., Michelsen, A., Minions, C., Oechel, W. C., Olefeldt, D., Parmentier, F.-J. W.,  
1023 Pirk, N., Poulter, B., Quinton, W., Rezanezhad, F., Risk, D., Sachs, T., Schaefer, K., Schmidt, N.  
1024 M., Schuur, E. A. G., Semenchuk, P. R., Shaver, G., Sonnentag, O., Starr, G., Treat, C. C.,  
1025 Waldrop, M. P., Wang, Y., Welker, J., Wille, C., Xu, X., Zhang, Z., Zhuang, Q., and Zona, D.:  
1026 Large loss of CO<sub>2</sub> in winter observed across the northern permafrost region, *Nat. Clim. Chang.*,  
1027 9, 852–857, <https://doi.org/10.1038/s41558-019-0592-8>, 2019.
- 1028 Novick, K. A., Biederman, J. A., Desai, A. R., Litvak, M. E., Moore, D. J. P., Scott, R. L., and  
1029 Torn, M. S.: The AmeriFlux network: A coalition of the willing, *Agric. For. Meteorol.*, 249,  
1030 444–456, <https://doi.org/10.1016/j.agrformet.2017.10.009>, 2018.
- 1031 Nykänen, H., Heikkinen, J. E. P., Pirinen, L., Tiilikainen, K., and Martikainen, P. J.: Annual  
1032 CO<sub>2</sub> exchange and CH<sub>4</sub> fluxes on a subarctic palsamire during climatically different years,  
1033 *Global Biogeochem. Cycles*, 17, 2003.
- 1034 Oechel, W. C., Vourlitis, G. L., Hastings, S. J., Zulueta, R. C., Hinzman, L., and Kane, D.:  
1035 Acclimation of ecosystem CO<sub>2</sub> exchange in the Alaskan Arctic in response to decadal climate  
1036 warming, *Nature*, 406, 978–981, <https://doi.org/10.1038/35023137>, 2000.
- 1037 Papale, D., Reichstein, M., Aubinet, M., Canfora, E., Bernhofer, C., Kutsch, W., Longdoz, B.,  
1038 Rambal, S., Valentini, R., Vesala, T., and Yakir, D.: Towards a standardized processing of Net  
1039 Ecosystem Exchange measured with eddy covariance technique: algorithms and uncertainty  
1040 estimation, *Biogeosciences*, 3, 571–583, <https://doi.org/10.5194/bg-3-571-2006>, 2006.
- 1041 Paris, J.-D., Ciais, P., Rivier, L., Chevallier, F., Dolman, H., Flaud, J.-M., Garrec, C., Gerbig, C.,  
1042 Grace, J., Huertas, E., Johannessen, T., Jordan, A., Levin, I., Papale, D., Valentini, R., Watson,  
1043 A., Vesala, T., and ICOS-PP Consortium: Integrated Carbon Observation System, 12397, 2012.
- 1044 Parker, T. C., Subke, J.-A., and Wookey, P. A.: Rapid carbon turnover beneath shrub and tree



- 1045 vegetation is associated with low soil carbon stocks at a subarctic treeline, *Glob. Chang. Biol.*,  
1046 21, 2070–2081, <https://doi.org/10.1111/gcb.12793>, 2015.
- 1047 Parmentier, F.-J., Sonnentag, O., Mauritz, M., Virkkala, A.-M., and Schuur, E.: Is the northern  
1048 permafrost zone a source or a sink for carbon?, *Eos*, 100, <https://doi.org/10.1029/2019eo130507>,  
1049 2019.
- 1050 Pastorello, G., Trotta, C., Canfora, E., Chu, H., Christianson, D., Cheah, Y.-W., Poindexter, C.,  
1051 Chen, J., Elbashandy, A., Humphrey, M., Isaac, P., Polidori, D., Ribeca, A., van Ingen, C.,  
1052 Zhang, L., Amiro, B., Ammann, C., Arain, M. A., Ardö, J., Arkebauer, T., Arndt, S. K., Arriga,  
1053 N., Aubinet, M., Aurela, M., Baldocchi, D., Barr, A., Beamesderfer, E., Marchesini, L. B.,  
1054 Bergeron, O., Beringer, J., Bernhofer, C., Berveiller, D., Billesbach, D., Black, T. A., Blanken,  
1055 P. D., Bohrer, G., Boike, J., Bolstad, P. V., Bonal, D., Bonnefond, J.-M., Bowling, D. R.,  
1056 Bracho, R., Brodeur, J., Brümmer, C., Buchmann, N., Burban, B., Burns, S. P., Buysse, P., Cale,  
1057 P., Cavagna, M., Cellier, P., Chen, S., Chini, I., Christensen, T. R., Cleverly, J., Collalti, A.,  
1058 Consalvo, C., Cook, B. D., Cook, D., Coursolle, C., Cremonese, E., Curtis, P. S., D’Andrea, E.,  
1059 da Rocha, H., Dai, X., Davis, K. J., De Cinti, B., de Grandcourt, A., De Ligne, A., De Oliveira,  
1060 R. C., Delpierre, N., Desai, A. R., Di Bella, C. M., di Tommasi, P., Dolman, H., Domingo, F.,  
1061 Dong, G., Dore, S., Duce, P., Dufrêne, E., Dunn, A., Dušek, J., Eamus, D., Eichelmann, U.,  
1062 ElKhidir, H. A. M., Eugster, W., Ewenz, C. M., Ewers, B., Famulari, D., Fares, S., Feigenwinter,  
1063 I., Feitz, A., Fensholt, R., Filippa, G., Fischer, M., Frank, J., Galvagno, M., Gharun, M.,  
1064 Gianelle, D., et al.: The FLUXNET2015 dataset and the ONEFlux processing pipeline for eddy  
1065 covariance data, *Sci Data*, 7, 225, <https://doi.org/10.1038/s41597-020-0534-3>, 2020.
- 1066 Pavelka, M., Acosta, M., Kiese, R., Altimir, N., Brümmer, C., Crill, P., Darenova, E., Fuß, R.,  
1067 Gielen, B., Graf, A., Klemmedtsson, L., Lohila, A., Longdoz, B., Lindroth, A., Nilsson, M.,  
1068 Maraňon-Jimenez, S., Merbold, L., Montagnani, L., Peichl, M., Pihlatie, M., Pumpanen, J.,  
1069 Ortiz, P. S., Silvennoinen, H., Skiba, U., Vestin, P., Weslien, P., Janouš, D., and Kutsch, W.:  
1070 Standardisation of chamber technique for CO<sub>2</sub>, N<sub>2</sub>O and CH<sub>4</sub> fluxes measurements from  
1071 terrestrial ecosystems, *Int. Agrophys.*, 32, 569–587, <https://doi.org/10.1515/intag-2017-0045>,  
1072 2018.
- 1073 Phillips, C. L., Bond-Lamberty, B., Desai, A. R., Lavoie, M., Risk, D., Tang, J., Todd-Brown,  
1074 K., and Vargas, R.: The value of soil respiration measurements for interpreting and modeling  
1075 terrestrial carbon cycling, *Plant Soil*, 413, 1–25, <https://doi.org/10.1007/s11104-016-3084-x>,  
1076 2017.
- 1077 Pirk, N., Sievers, J., Mertes, J., Parmentier, F.-J. W., Mastepanov, M., and Christensen, T. R.:  
1078 Spatial variability of CO<sub>2</sub> uptake in polygonal tundra: assessing low-frequency disturbances in  
1079 eddy covariance flux estimates, *Biogeosciences*, 14, 3157–3169, <https://doi.org/10.5194/bg-14-3157-2017>, 2017.
- 1081 Reynolds, M. K., Walker, D. A., Balser, A., Bay, C., Campbell, M., Cherosov, M. M., Daniëls,  
1082 F. J. A., Eidesen, P. B., Ermokhina, K. A., Frost, G. V., Jedrzejek, B., Jorgenson, M. T.,  
1083 Kennedy, B. E., Kholod, S. S., Lavrinenko, I. A., Lavrinenko, O. V., Magnússon, B., Matveyeva,  
1084 N. V., Metúsalemsson, S., Nilsen, L., Olthof, I., Pospelov, I. N., Pospelova, E. B., Pouliot, D.,  
1085 Razzhivin, V., Schaepman-Strub, G., Šibík, J., Telyatnikov, M. Y., and Troeva, E.: A raster



- 1086 version of the Circumpolar Arctic Vegetation Map (CAVM), *Remote Sens. Environ.*, 232,  
1087 111297, <https://doi.org/10.1016/j.rse.2019.111297>, 2019.
- 1088 Reichstein, M., Falge, E., Baldocchi, D., Papale, D., Aubinet, M., Berbigier, P., Bernhofer, C.,  
1089 Buchmann, N., Gilmanov, T., Granier, A., Grunwald, T., Havrankova, K., Ilvesniemi, H.,  
1090 Janous, D., Knohl, A., Laurila, T., Lohila, A., Loustau, D., Matteucci, G., Meyers, T., Miglietta,  
1091 F., Ourcival, J.-M., Pumpanen, J., Rambal, S., Rotenberg, E., Sanz, M., Tenhunen, J., Seufert,  
1092 G., Vaccari, F., Vesala, T., Yakir, D., and Valentini, R.: On the separation of net ecosystem  
1093 exchange into assimilation and ecosystem respiration: review and improved algorithm, *Glob.*  
1094 *Chang. Biol.*, 11, 1424–1439, <https://doi.org/10.1111/j.1365-2486.2005.001002.x>, 2005.
- 1095 Riutta, T., Laine, J., Aurela, M., Rinne, J., Vesala, T., Laurila, T., Haapanala, S., Pihlatie, M.,  
1096 and Tuittila, E.-S.: Spatial variation in plant community functions regulates carbon gas dynamics  
1097 in a boreal fen ecosystem, *Tellus B Chem. Phys. Meteorol.*, 59, 838–852,  
1098 <https://doi.org/10.1111/j.1600-0889.2007.00302.x>, 2007.
- 1099 Ryan, M. G., Lavigne, M. B., and Gower, S. T.: Annual carbon cost of autotrophic respiration in  
1100 boreal forest ecosystems in relation to species and climate, *J. Geophys. Res.*, 102, 28871–28883,  
1101 <https://doi.org/10.1029/97jd01236>, 1997.
- 1102 Schuur, E. A. G., McGuire, A. D., Schädel, C., Grosse, G., Harden, J. W., Hayes, D. J.,  
1103 Hugelius, G., Koven, C. D., Kuhry, P., Lawrence, D. M., Natali, S. M., Olefeldt, D.,  
1104 Romanovsky, V. E., Schaefer, K., Turetsky, M. R., Treat, C. C., and Vonk, J. E.: Climate change  
1105 and the permafrost carbon feedback, *Nature*, 520, 171–179, <https://doi.org/10.1038/nature14338>,  
1106 2015.
- 1107 Sellers, P. J., Hall, F. G., Kelly, R. D., Black, A., Baldocchi, D., Berry, J., Ryan, M., Ranson, K.  
1108 J., Crill, P. M., Lettenmaier, D. P., Margolis, H., Cihlar, J., Newcomer, J., Fitzjarrald, D., Jarvis,  
1109 P. G., Gower, S. T., Halliwell, D., Williams, D., Goodison, B., Wickland, D. E., and Guertin, F.  
1110 E.: BOREAS in 1997: Experiment overview, scientific results, and future directions, *J. Geophys.*  
1111 *Res.*, 102, 28731–28769, <https://doi.org/10.1029/97jd03300>, 1997.
- 1112 Shaver, G. R., L. E. Street, Rastetter, E. B., M. T. Van Wijk, and Williams, M.: Functional  
1113 Convergence in Regulation of Net CO<sub>2</sub> Flux in Heterogeneous Tundra Landscapes in Alaska and  
1114 Sweden, *J. Ecol.*, 95, 802–817, 2007.
- 1115 Siewert, M. B., Hanisch, J., Weiss, N., Kuhry, P., Maximov, T. C., and Hugelius, G.: Comparing  
1116 carbon storage of Siberian tundra and taiga permafrost ecosystems at very high spatial  
1117 resolution: ECOSYSTEM CARBON IN TAIGA AND TUNDRA, *J. Geophys. Res. Biogeosci.*,  
1118 120, 1973–1994, <https://doi.org/10.1002/2015jg002999>, 2015.
- 1119 Soloway, A. D., Amiro, B. D., Dunn, A. L., and Wofsy, S. C.: Carbon neutral or a sink?  
1120 Uncertainty caused by gap-filling long-term flux measurements for an old-growth boreal black  
1121 spruce forest, *Agric. For. Meteorol.*, 233, 110–121,  
1122 <https://doi.org/10.1016/j.agrformet.2016.11.005>, 2017.
- 1123 Tarnocai, C., Canadell, J. G., Schuur, E. A. G., Kuhry, P., Mazhitova, G., and Zimov, S.: Soil  
1124 organic carbon pools in the northern circumpolar permafrost region, *Global Biogeochem. Cycles*,



- 1125 23, 2009.
- 1126 Tramontana, G., Migliavacca, M., Jung, M., Reichstein, M., Keenan, T. F., Camps-Valls, G.,  
1127 Ogee, J., Verrelst, J., and Papale, D.: Partitioning net carbon dioxide fluxes into photosynthesis  
1128 and respiration using neural networks, *Glob. Chang. Biol.*, 26, 5235–5253,  
1129 <https://doi.org/10.1111/gcb.15203>, 2020.
- 1130 Valentini, R.: EUROFLUX: An Integrated Network for Studying the Long-Term Responses of  
1131 Biospheric Exchanges of Carbon, Water, and Energy of European Forests, in: *Fluxes of Carbon,  
1132 Water and Energy of European Forests*, edited by: Valentini, R., Springer Berlin Heidelberg,  
1133 Berlin, Heidelberg, 1–8, [https://doi.org/10.1007/978-3-662-05171-9\\_1](https://doi.org/10.1007/978-3-662-05171-9_1), 2003.
- 1134 Virkkala, A.-M., Virtanen, T., Lehtonen, A., Rinne, J., and Luoto, M.: The current state of CO<sub>2</sub>  
1135 flux chamber studies in the Arctic tundra: A review, *Progress in Physical Geography: Earth and  
1136 Environment*, 42, 162–184, <https://doi.org/10.1177/0309133317745784>, 2018.
- 1137 Virkkala, A.-M., Abdi, A. M., Luoto, M., and Metcalfe, D. B.: Identifying multidisciplinary  
1138 research gaps across Arctic terrestrial gradients, *Environ. Res. Lett.*, 14, 124061,  
1139 <https://doi.org/10.1088/1748-9326/ab4291>, 2019.
- 1140 Virkkala, A.-M., Natali, S., Rogers, B. M., Watts, J. A., Savage, K., Connon, S. J., Mauritz, M.,  
1141 Schuur, E. A. G., Peter, D., and Minions, C. et al.: The ABCflux Database: Arctic-Boreal CO<sub>2</sub>  
1142 Flux Observations Aggregated to Monthly Time Steps, ORNL DAAC, Oak Ridge, Tennessee,  
1143 USA, <https://doi.org/10.3334/ORNLDAAAC/1934>, 2021a.
- 1144 Virkkala, A.-M., Aalto, J., Rogers, B. M., Tagesson, T., Treat, C. C., Natali, S. M., Watts, J. D.,  
1145 Potter, S., Lehtonen, A., Mauritz, M., Schuur, E. A. G., Kochendorfer, J., Zona, D., Oechel, W.,  
1146 Kobayashi, H., Humphreys, E., Goeckede, M., Iwata, H., Lafleur, P. M., Euskirchen, E. S.,  
1147 Bokhorst, S., Marushchak, M., Martikainen, P. J., Elberling, B., Voigt, C., Biasi, C., Sonnentag,  
1148 O., Parmentier, F.-J. W., Ueyama, M., Celis, G., St Loius, V. L., Emmerton, C. A., Peichl, M.,  
1149 Chi, J., Järveoja, J., Nilsson, M. B., Oberbauer, S. F., Torn, M. S., Park, S.-J., Dolman, H.,  
1150 Mammarella, I., Chae, N., Poyatos, R., López-Blanco, E., Røjle Christensen, T., Jung Kwon, M.,  
1151 Sachs, T., Holl, D., and Luoto, M.: Statistical upscaling of ecosystem CO<sub>2</sub> fluxes across the  
1152 terrestrial tundra and boreal domain: regional patterns and uncertainties, *Glob. Chang. Biol.*,  
1153 <https://doi.org/10.1111/gcb.15659>, 2021b.
- 1154 Voigt, C., Lamprecht, R. E., Marushchak, M. E., Lind, S. E., Novakovskiy, A., Aurela, M.,  
1155 Martikainen, P. J., and Biasi, C.: Warming of subarctic tundra increases emissions of all three  
1156 important greenhouse gases - carbon dioxide, methane, and nitrous oxide, *Glob. Chang. Biol.*,  
1157 23, 3121–3138, <https://doi.org/10.1111/gcb.13563>, 2017.
- 1158 Wang, K., Liu, C., Zheng, X., Pihlatie, M., Li, B., Haapanala, S., Vesala, T., Liu, H., Wang, Y.,  
1159 Liu, G., and Hu, F.: Comparison between eddy covariance and automatic chamber techniques for  
1160 measuring net ecosystem exchange of carbon dioxide in cotton and wheat fields, *Biogeosciences*,  
1161 10, 6865–6877, <https://doi.org/10.5194/bg-10-6865-2013>, 2013.
- 1162 Wang, L., Lee, X., Wang, W., Wang, X., Wei, Z., Fu, C., Gao, Y., Lu, L., Song, W., Su, P., and  
1163 Lin, G.: A Meta-Analysis of Open-Path Eddy Covariance Observations of Apparent CO<sub>2</sub> Flux in

<https://doi.org/10.5194/essd-2021-233>  
Preprint. Discussion started: 28 July 2021  
© Author(s) 2021. CC BY 4.0 License.



1164 Cold Conditions in FLUXNET, *J. Atmos. Ocean. Technol.*, 34, 2475–2487,  
1165 <https://doi.org/10.1175/JTECH-D-17-0085.1>, 2017.

1166